

# Supervision-free Vision-Language Alignment

Giorgio Giannone  
Amazon

Ruoteng Li  
Amazon

Qianli Feng  
Amazon

Evgeny Perevodchikov  
Amazon

Rui Chen  
Amazon

Alex M Martinez  
Amazon

## Abstract

Vision-language models (VLMs) have demonstrated remarkable potential in integrating visual and linguistic information, but their performance is often constrained by the need for extensive, high-quality image-text training data. Curation of these image-text pairs is both time-consuming and computationally expensive. To address this challenge, we introduce SVP (Supervision-free Visual Projection), a novel framework that enhances vision-language alignment without relying on curated data or preference annotation. SVP leverages self-captioning and a pre-trained grounding model as a feedback mechanism to elicit latent information in VLMs. We evaluate our approach across six key areas: captioning, referring, visual question answering, multitasking, hallucination control, and object recall. Results demonstrate significant improvements, including a 14% average improvement in captioning tasks, up to 12% increase in object recall, and substantial reduction in hallucination rates. Notably, a small VLM using SVP achieves hallucination reductions comparable to a model five times larger, while a VLM with initially poor referring capabilities more than doubles its performance, approaching parity with a model twice its size.

## 1. Introduction

Vision-Language Models (VLMs [12, 120]) are essential to deploying expert level artificial intelligence, as human intelligence is predominantly multimodal.

Generative VLMs [17, 52, 53, 111] built upon Large Language Models (LLMs) have shown great promises in zero-shot abilities on various downstream vision-linguistic tasks (Fig. 2.(iv)), unlocking new multimodal capacities and providing powerful generalization to specialized machine

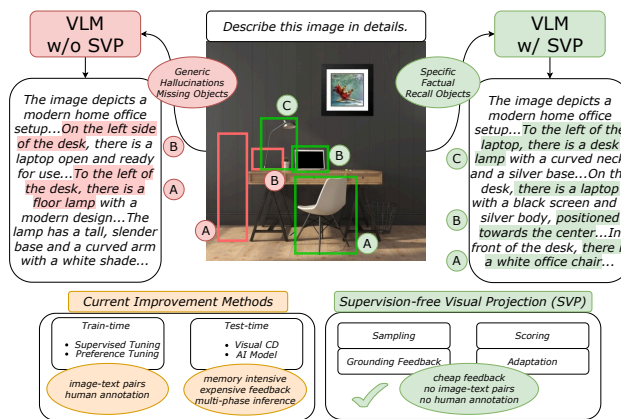


Figure 1. **Improving Vision-Language Alignment.** Vision-language models (VLMs) often produce descriptions that lack specificity and accuracy, frequently hallucinating objects not present in the image or failing to mention important elements that are actually there (left side). Our approach, *Supervision-free Visual Projection* (SVP), addresses these shortcomings leveraging self-captioning and grounding feedback. SVP projects visual information into language space, enhancing vision-language alignment without relying on time-consuming human annotations, curated image-text pairs, or expensive AI feedback (right side). As a result, we achieve models with greater contextual relevance, fewer hallucinations, and enhanced object recall. These improvements pave the way for more accurate and reliable VLMs. See Appendix Fig. 10 for more details.

learning models. By learning a mapping between linguistic tokens and visual features, such VLMs enjoy the strong generation capabilities of LLMs [14, 98] and the understanding of the physical world of computer vision models [25, 77].

However, VLMs derived from pretrained backbones are known to be impacted by the hallucinations and biases from LLMs [79, 82]. It is frequently observed that these VLMs

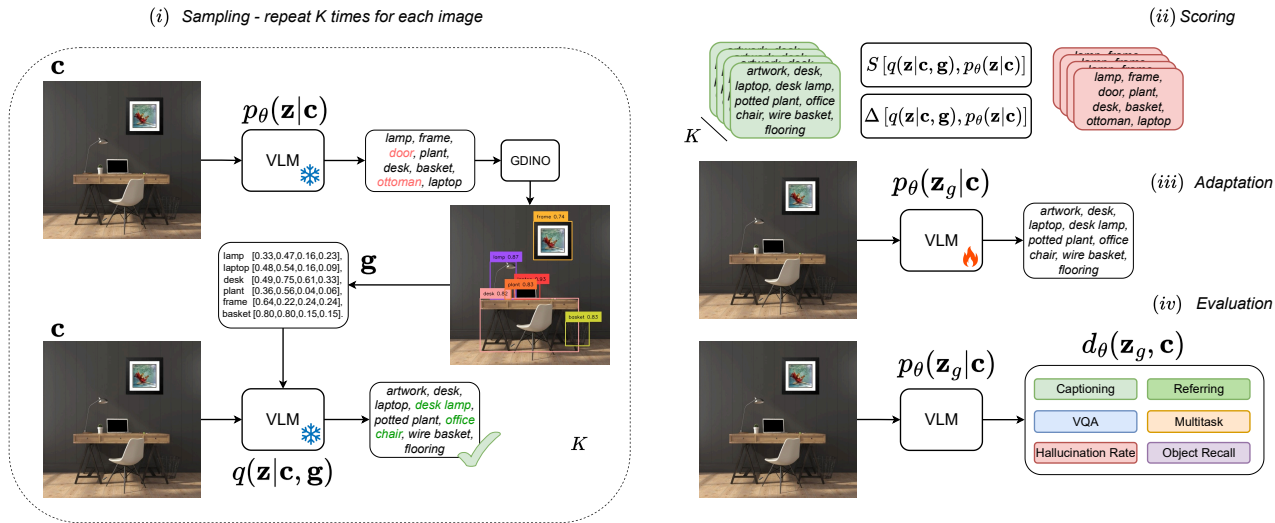


Figure 2. **Overview of SVP.** The inner-loop (left) generates  $K$  samples per input  $C$  with and without grounding, then scores and ranks them, selecting the top 20% (right side). Instead of visually representing the grounding, we transform it into textual form and incorporate it into the prompt as context. This process includes (i) data generation with grounding feedback and (ii) sample scoring. The outer-loop (right) uses selected samples to (iii) adapt the base model. Post-SVP adaptation, we evaluate on ten benchmarks and six tasks (iv). Full VLM output in Appendix Fig. 10. Prompt structure in Appendix F.

fail to produce text consistent with the visual content (left side Fig. 1), i.e., the generated text describes entities not present in the input image or misses relevant entities altogether, generating content not grounded in the visual input [7, 21]. Addressing these shortcomings is crucial for future deployment of VLMs in high-stakes, real-world applications across the frontiers of scientific discovery [35] and engineering [74, 91].

Researchers have explored various approaches to solve the above problem in VLMs (bottom Fig. 1). Most of these works focus on fine-tuning VLMs with supervised (carefully curated) data to improve grounding [11, 73, 113, 115, 122] and vision-language alignment [60, 93]. Unfortunately, this data approach tends to be costly and sample-inefficient, requiring large amounts of image-text annotations even for small models to resolve the above stated problem [115]. Preference-based post-training methods [20, 69, 78] as another popular approach align VLM outputs with visual inputs [93, 125] but require curated preference pairs [26, 93]. And, test-time approaches [26, 51, 102, 112] improve grounding without architectural changes, yet their computational demands and model-specific heuristics limit broad applicability.

To address the significant challenges posed by the extensive data and annotation requirements of modern VLMs, we propose to leverage external feedback to enhance the alignment between visual and linguistic modalities in a task-agnostic manner (right side Fig. 1).

*Drawing inspiration from human learning, we propose*

*to emulate the way humans efficiently align sensory experiences with language by grounding new information in tangible visual examples leveraging feedback [34, 95, 96]. We hypothesize that spatial and positional reasoning is the key for connecting the low-level visual elements and high-level linguistic representations [68, 72, 99], and that an external visual grounding model [63], agnostic to the VLM’s shortcomings, can be used as feedback to extract latent information in the models.*

Specifically, in this work, we introduce SVP (*Supervision-free Visual Projection*, Fig. 2), an algorithm founded on two core principles: self-improvement and grounding feedback. The self-improvement approach [5, 32, 117] utilizes the model’s own outputs to enhance its performance. And, the grounding feedback provides the VLM with a mechanism to improve its output and select informative samples. Our goal is not to directly build a specialist grounding model, but to *leverage grounding as feedback to elicit latent information in the model*, with the aim of better aligning language and visual representations without the need of costly image-text annotations [73, 93], preference data [69, 78], or multi-step inference workflows [102, 112].

SVP is a three-step process:

- (i) *Inner-Loop Sampling:* A base VLM generates detailed and comprehensive image descriptions. These descriptions are then processed by a small pre-trained grounding model [63]. The resulting spatially enriched grounding output serves as feedback, conditioning the same VLM to generate text tokens that better align with the visual

information (Fig. 2.(i)).

- (ii) *Scoring*: This step employs a scoring and ranking mechanism to select grounded samples that are more informative and better aligned with the visual input (Fig. 2.(ii)).
- (iii) *Outer-Loop Adaptation*: The base VLM undergoes adaptation [39] on the filtered dataset. Importantly, the grounding information is not shown during the fine-tuning process but is utilized during inference (Fig. 2.(iii)).

**Contributions** Our contributions are the following:

- We introduce *Supervision-free Visual Projection (SVP)*, a novel, general-purpose method that enhances the alignment between textual and visual representations in VLMs. This approach leverages self-captioning and visual grounding techniques to improve multimodal understanding.
- SVP operates without the need for manual annotations, relying solely on a small grounding model as external feedback. Its model-agnostic design ensures easy applicability across various modern VLM frameworks.
- We present comprehensive experimental results across 10 diverse vision-language benchmarks, including captioning, referring expressions, visual question answering, multi-task performance, hallucination control, and object recall, demonstrating the effectiveness of our approach.

## 2. Related Work

**Improving Vision-Language Models** Enhancing vision-language alignment in VLMs is an active research area. Explicit grounding in generative VLMs [17, 52, 53] has primarily addressed hallucinations [26, 102]. Common strategies include incorporating grounding annotations into training data [73] for vision-centric VLMs [11, 113, 115, 122], though this process is costly and error-prone. Explicit supervision during fine-tuning can enhance alignment [60, 93] but requires extensive high-quality data. Techniques like RLHF [69] and DPO [78], originally for LLMs, have been adapted to align VLM outputs with visual inputs [93, 125, 127]. These post-training approaches incorporate feedback [26, 93] but are limited by the need for reward signals and curated preference pairs. Test-time methods [102], such as Visual Contrastive Decoding [51] and Multi-Modal Mutual-Information Decoding [26], aim to improve grounding at inference without altering model architecture or training. Woodpecker [112] proposes a five-step inference procedure to mitigate hallucination. While effective, these methods often require memory-intensive computation and model-specific heuristics, limiting their usage.

**Grounding Models** Visual grounding, the dual of text-image alignment, organizes information within VLMs, aligning visual and textual modalities in both representation and

generation. The concept of grounding has deep roots in cognitive sciences [4, 9, 29, 47]. In the context of computer vision, visual grounding can be seen as an extension of the classic closed-set detection problem [16, 28, 80, 121]. Traditional object detection, using curated datasets [59], has improved precision and speed but struggles with scaling to larger class sets and varying detection granularity’s [23, 33]. Visual grounding inverts this approach, using class sets as input to assign bounding boxes, generalizing to accommodate various textual inputs. Contrastive models like GLIP [55] and GroundingDINO [63] offer flexible, generalized detection models, enhancing spatial understanding [112] and supporting diverse tasks. Auto-regressive VLMs have further expanded capabilities in grounding and referring tasks [73, 97, 113, 115], bridging visual and linguistic information more effectively.

## 3. Method

### 3.1. Preliminaries

**Notation** We use  $p(\mathbf{x}|\mathbf{c})$  and  $p(\mathbf{z}|\mathbf{c})$  to denote auto-regressive distributions for simplicity. Here,  $\mathbf{c}$  is the conditioning information (image and prompt inputs),  $\mathbf{z}$  is a model sample or visual projection using grounding feedback, and  $\mathbf{x}$  is the model’s task-specific output. These distributions are shorthand for:  $p(\mathbf{x}|\mathbf{c}) = p(\mathbf{x}_T|\mathbf{c}) \prod_{t=1}^T p(\mathbf{x}_{t-1}|\mathbf{x}_t, \mathbf{c})$ . Similarly for  $p(\mathbf{z}|\mathbf{c})$ . In  $p(\mathbf{x}|\mathbf{z}, \mathbf{c})$ ,  $\mathbf{z}$  represents sampling trajectories  $\mathbf{z}_{1:T_z}$ . The conditioning information  $\mathbf{c}$  is typically a given input to the model.

Given a context  $\mathbf{c} = (\mathbf{c}_v, \mathbf{c}_t)$ , where  $\mathbf{c}_v$  is the visual input and  $\mathbf{c}_t$  is a textual prompt, we write a Visual Projection (VP) as  $p(\mathbf{z}|\mathbf{c})$ , where  $\mathbf{z}$  is a comprehensive language-based representation for the visual input. When conditioning on grounding information  $\mathbf{g}$ , we write a grounded VP as  $q(\mathbf{z}|\mathbf{c}, \mathbf{g})$ . The conditional entropy is defined as  $\mathbb{H}[\mathbf{z}|\mathbf{c}] = -\sum_{\mathbf{z}} p(\mathbf{z}|\mathbf{c}) \log p(\mathbf{z}|\mathbf{c})$ .

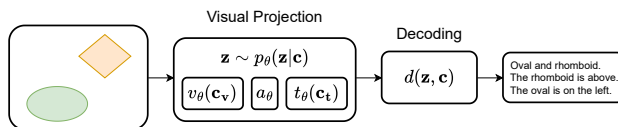


Figure 3. Vision-Language Generative Model.

**Vision-Language Models** Generative VLMs are versatile multimodal models that process text and images together. LLaVA-like models (Fig. 3) comprise a visual encoder  $v_\theta(\mathbf{c}_v)$ , a text encoder  $t_\theta(\mathbf{c}_t)$ , an adapter  $a_\theta$  aligning visual output to text, and a large language model. The model  $p_\theta$  uses the conditioning  $\mathbf{c}$  to generate token trajectories  $\mathbf{z}$ , which are then decoded for various tasks. These models undergo multi-phase training: multimodal pre-training, visual-

text alignment, and visual instruction-tuning [53, 61, 126]. This process enables VLMs to leverage their cross-modal capabilities across a wide range of applications.

**Vision-Language Grounding** Grounding matches language descriptions to spatial regions in visual information. A grounding model  $g(\mathbf{z}, \mathbf{c}_v)$  processes visual  $\mathbf{c}_v$  and textual  $\mathbf{z}$  inputs, producing open-set detections as labels and bounding boxes (Fig. 4). While traditional object detection involves

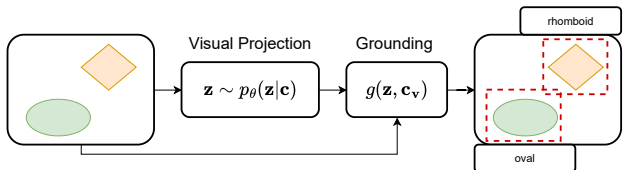


Figure 4. Vision-Language Grounding.

multi-class classification and bounding box regression, models like GLIP and GroundingDINO re-frame it as grounding with predefined textual descriptors. As specialized VLMs, grounding models provide flexibility for a range of applications, including tasks like detection and placement.

### 3.2. Supervision-free Visual Projection

The core idea behind *SVP* is to generate a task-agnostic language-based representation  $\mathbf{z}$ , referred as *Visual Projection* (VP), for the visual input  $\mathbf{c}$ , utilizing sampling and grounding (Fig. 2.(i)). VPs function as latent variables or generalized captions (Fig. 1). *SVP* aims to refine these VPs through self-improving iterative methods, drawing inspiration from techniques designed to elicit reasoning in language models [36, 105, 117, 118], and posterior inference in latent variable models [43] (See Appendix E and Appendix G for more details). The goal of *SVP* is to strengthen the alignment between vision and language modalities, thereby improving the performance of the base VLM across a wide range of tasks.

**Grounding as Posterior Inference** VLMs are built using discrete tokens [100]. We assume the VPs are tokenized following a multinomial distribution, and re-write:

$$p_\theta(\mathbf{x}|\mathbf{c}) = \sum_{\mathbf{z}} p_\theta(\mathbf{x}|\mathbf{z}, \mathbf{c}) p_\theta(\mathbf{z}|\mathbf{c}), \quad (1)$$

where  $\mathbf{c}$  is the conditioning,  $\mathbf{z}$  is a sample from the model  $p_\theta$  with trainable parameters  $\theta$ , and  $\mathbf{x}$  is the model output.

Our goal is to provide feedback to the model to better ground the language output in the visual input. A simple option is to define a posterior  $q(\mathbf{z}|\mathbf{c}, \mathbf{g})$ , where  $\mathbf{g}$  is the external feedback, for example provided by a small pre-trained grounding model  $g(\mathbf{z}, \mathbf{c}_v)$  (Fig. 4). Introducing posterior

inference for Eq. (1), we can define a variational lower-bound [43, 48] of the form:

$$\mathbb{E}_{q(\mathbf{z}|\mathbf{c}, \mathbf{g})} [\log p_\theta(\mathbf{x}, \mathbf{z}|\mathbf{c}) - \log q(\mathbf{z}|\mathbf{c}, \mathbf{g})]. \quad (2)$$

For many practical applications, we can approximate  $p_\theta(\mathbf{x}|\mathbf{z}, \mathbf{c})$  with a deterministic decoder,  $d(\mathbf{z}, \mathbf{c})$ .

The bound defined in Eq. (2), while challenging to train for a VLM/LLM [36, 66], is straightforward to evaluate [49]. This insight reveals a promising approach to enhance VLM sampling: utilizing the bound to construct a scoring mechanism that effectively leverage grounding signal (Fig. 2.(i)).

**Sampling** For a given input  $\mathbf{c}$ , the process involves executing the posterior  $q(\mathbf{z}|\mathbf{c}, \mathbf{g})$  with grounding feedback  $\mathbf{g}$  and generating logits for each element  $v$  in the vocabulary  $V$  and each generated token  $t$  in the sequence  $T$ . Concurrently, the base model is run to perform the same computations over  $\mathbf{c}$ , obtaining the prior  $p_\theta(\mathbf{z}|\mathbf{c})$ . By comparing the posterior and prior distributions, we can quantify the grounding effect, providing insights into how visual context influences the model’s predictions.

**Scoring** Following such intuition, we build a scoring of the form (Fig. 2.(ii)):

$$S[q, p] = \sum_t \gamma_t \sum_v S_{v,t}[q, p], \quad (3)$$

$$S_{v,t}[q, p] = w_{v,t} [\log q_{v,t} - \log p_{\theta_{v,t}}],$$

where  $\gamma_t \in [0, 1]$  accounts for sequence length and  $w_{v,t}$  is a re-weighting factor (Fig. 5 and Appendix E). Image-text pairs  $(\mathbf{c}, \mathbf{z})$  with high score based on Eq. (3) are collected and used to fine-tune the base model (Fig. 2). The underlying assumption is that, within a specific model, substantial discrepancies between  $q$  and  $p$  are primarily attributed to the grounding conditioning  $\mathbf{g}$ . These discrepancies are expected to provide the most valuable information for the base VLM (Fig. 5).

Low values of  $S[q, p]$  indicate token trajectories that are known by the base model  $p$ , offering little learning potential. Conversely, high values of  $S[q, p]$  signify trajectories that deviate from the base model’s expectations across the vocabulary. These "surprising" trajectories are likely to provide valuable feedback and novel information [15, 37, 71], enhancing the vision-language alignment in the base VLM.

It is crucial to note that generic, unconditional surprise - samples rich in information from an entropy perspective [87] - does not inherently enhance a VLM’s performance. Our working hypothesis posits that if the grounding conditioning is truly informative, surprising instances will contribute to the model’s learning process statistically. This assumption underpins our strategy of utilizing grounding and scoring mechanisms to improve the model.

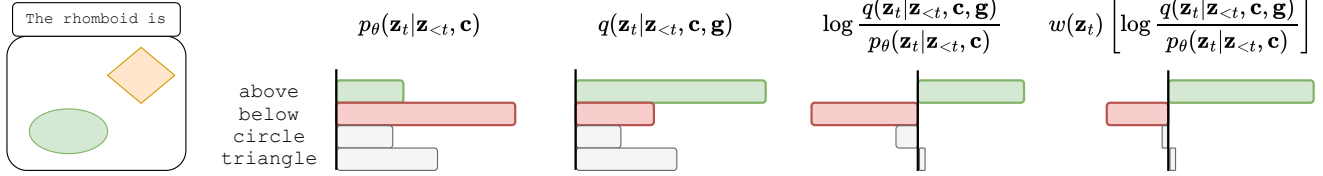


Figure 5. **Visualization of prior and posterior distribution** for token  $t$  over a reduced vocabulary  $V = \{\text{above, below, circle, rhomboid}\}$ . Without grounding feedback, the model  $p_\theta$  incorrectly assigns high likelihood to the wrong spatial relationship between the circle and rhomboid (`below`). By incorporating grounding as feedback through  $q$ , the model successfully assigns higher likelihood to the correct token (`above`). We then apply a log-ratio and re-weighting using the feedback-based distribution, where  $w(\mathbf{z}_t) \propto q(\mathbf{z}_t | \mathbf{z}_{<t}, \mathbf{c}, \mathbf{g})$ . This approach effectively reduces the weight of irrelevant tokens (which are weighted similarly in both distributions) while emphasizing tokens deemed relevant by the grounded distribution  $q$ .

Using similar reasoning, we define a score function based on entropy differentials [67] as

$$\Delta[q, p] = - \sum_{v,t} p_{\theta_{v,t}} \log p_{\theta_{v,t}} + \sum_{v,t} q_{v,t} \log q_{v,t}. \quad (4)$$

This score function is built based on our assumption that the grounded conditional entropy  $\mathbb{H}[\mathbf{z} | \mathbf{c}, \mathbf{g}]$  increases the information provided to the model. In other words, we assume that  $\mathbb{H}[\mathbf{z} | \mathbf{c}, \mathbf{g}] < \mathbb{H}[\mathbf{z} | \mathbf{c}]$ , as  $\mathbf{g}$  should encode information that aids in describing  $\mathbf{c}$ .

Leveraging such scores, we can construct a system to rank sequence trajectories generated by conditionally grounded VLMs. Specifically, we score posterior sequences  $\mathbf{z}_q$  (Appendix Fig. 20b) using  $S[q, p]$  or  $\Delta[q, p]$ , rank them, and select the top  $k$ . These entropy and divergence-based scores typically provide similar signals for grounding and diversity (Appendix Fig. 20a).

**SVP** SVP consists of three main phases to learn a better VP from the grounding feedback: (i) sampling from the VLM using grounding; (ii) scoring and filtering the samples; and (iii) adapting the VLM. Borrowing from the meta-learning literature [38], we refer to the sampling phase as the inner-loop, and to the adaptation phase as the outer-loop (see Fig. 2 and algorithm 1). More details in Appendix E.

**Inner-loop** The process begins with the selection of  $C$  input natural images (Fig. 2.(i)). For each input prompt  $\mathbf{c}$  (comprising both image and text), the algorithm samples  $K$  sequences  $\mathbf{z}$  from the base VLM  $p_\theta(\mathbf{z} | \mathbf{c})$ . It then applies the grounding model  $g(\mathbf{z}, \mathbf{c}_v)$  to  $\mathbf{z}$  and the visual input  $\mathbf{c}_v$ , yielding the grounding conditioning  $\mathbf{g}$ , consisting of a set of noun phrases extracted from  $\mathbf{z}$  and corresponding bounding boxes. Subsequently,  $K$  posterior sequences  $\mathbf{z}_g$  are sampled from the grounded model  $q(\mathbf{z} | \mathbf{c}, \mathbf{g})$ . Then samples are scored (Fig. 2.(ii)) and ranked according to  $S(q, p_\theta)$  or  $\Delta(q, p)$ , and the top  $k$  samples  $\mathbf{z}_g^k$  are retained.

**Outer-loop** This is the optimization phase (Fig. 2.(iii)), where SVP adapts the base model using self-generated visual projections and grounding feedback. The top-scoring samples  $\mathbf{z}_g^k$  from the inner-loop are used to fine-tune the model on input images  $C$  and their corresponding generated text outputs. We employ standard cross-entropy loss for next token prediction [76] to update the base VLM’s parameters  $\theta$ . Given the limited sample size, we utilize parameter-efficient fine-tuning [39].

The full SVP process can be repeated for  $I$  iterations, progressively refining the base VLM’s alignment with the grounded VLM (Fig. 9a). Notably, our results demonstrate that even a single iteration of SVP significantly enhances the model’s performance on key tasks, underscoring SVP’s effectiveness in improving vision-language alignment and downstream tasks in VLMs.

## 4. Experiments

**Seed Images and Models** We utilize a pre-trained grounding model [63] to provide the external feedback signals. For our core experiments, we randomly sampled a subset of  $C = 1000$  natural images from the COCO2014 training set [59]. We conduct a comprehensive comparison against various baselines, including models fine-tuned with self-captioning without grounding and preference-based adaptation methods. Our evaluation encompasses a wide range of model scales (.5, 7, 8, 13, 19, 40 billion parameters), architectures (LLaVA-1.5 [60], LLaVA-1.6 [61], LLaVA-OV [52], VILA [58], InternVL [18]), visual encoders (CLIP [77], SigLIP [119], ViT [25]), language encoders (Vicuna [19], Mistral [42], Qwen2 [109], Yi-2 [114]), and scoring mechanisms  $S(q, p)$  and  $\Delta(q, p)$ .

**Implementation Details** We propose two variants of our approach: SVP (C) and SVP (CVQ). The former leverages only grounded self-generated captions, while the latter incor-

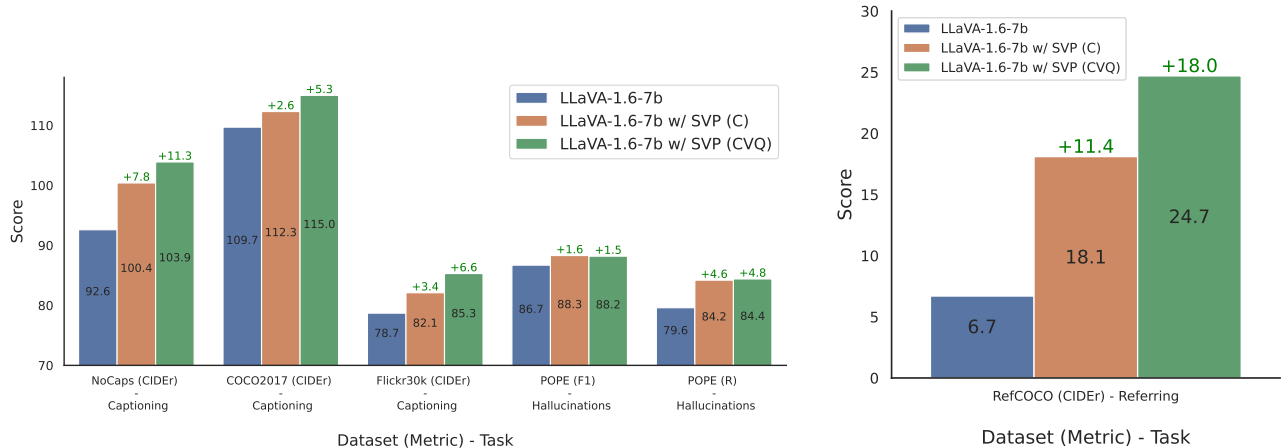


Figure 6. **Benchmark Results** for Captioning (CIDEr), Referring (CIDEr), Hallucination control (F1), and Object Recall (R) for base VLM (LLaVA-1.6-7b) and VLM adapted using our method *SVP*. Higher is better for all the tasks, datasets, and metrics. The VLM demonstrates improved performance across a range of key multimodal tasks like image captioning, referring expression comprehension, and hallucination control when adapted using the *SVP* technique. We adapt the model on COCO2014 [59] train set images, using self-captioning and GroundingDINO [63] as feedback signals. While captioning and referring saw clear gains, multitasking and visual question answering remained largely stable. Notably, there was a significant reduction in hallucinations compared to the base model. These results provide evidence that grounding as feedback can be leveraged to elicit latent knowledge in the model and improve visual-language alignment. More detailed in Tab. 1 and Appendix Fig. 6.

porates additional visual queries. These visual queries are questions the model encountered during training. By prompting the model to answer again these queries, we mitigate the risk of over-specialization on description-based tasks.

In the *SVP* inner-loop, we sample  $K = 20$  per image from base and grounded VLMs, selecting the top 20% using Eqs. (3) and (4). For  $C = 1000$ , we select 4000 samples for *SVP* (C) and add an equal number of visual queries for *SVP* (CVQ), totaling 8000 self-generated pairs. This is smaller than supervised multimodal fine-tuning datasets but sufficient to influence model behavior [93, 127]. We use normalized  $x_1y_1x_2y_2$  bounding box format. Degenerate samples ( $< 0.5\%$  for LLaVA-1.5/1.6,  $\approx 5\%$  for LLaVA-OV) are removed before scoring and filtering. We set  $\gamma_t = 1$  and  $w_{v,t} = q_{v,t}$ .

In the outer-loop, we fine-tune using LoRa [39] ( $\alpha = 16$ ,  $r = 64$  for  $\leq 7b$  models;  $\alpha = 256$ ,  $r = 128$  for 13b models) for one epoch. Experiments use 8-A100 GPUs with batch size  $B = 20$ . We follow default settings from [52, 61], running *SVP* for up to  $I = 3$  iterations. We re-evaluate LLaVA versions ( $\leq 13b$ ) on benchmarks without LLM-based evaluation, performing sample-wise, zero-shot evaluations without prompt engineering or batching to avoid model-specific artifacts.

**Metrics** We use the CIDEr score [101] for captioning and referring tasks; accuracy for VQA and multitasking. F1, Accuracy and Recall for hallucination and object recall. We also consider standard metrics for language translation like

BLEU [70], METEOR [8], and ROUGE [57] scores. We re-compute metrics for LLaVA baselines and variants (1.5, 1.6, OV) up to 13b parameters.

#### 4.1. Vision-Language Benchmarks

**Datasets** We evaluate *SVP* on 6 tasks and 10 core benchmarks for VLMs: we consider COCO2017 [59], NoCaps [2], and Flickr30k [75] for generative captioning; RefCOCO [46], RefCOCO+, RefCOCog for referring expression generation, ScienceQA [81], VQAv2 [30] and GQA [40] for visual question answering. We use MMBench [64] and MMMU [116] for multitasking and POPE [56] for hallucination and object recall. Given the large amount of models and tasks considered, we use the *lite* evaluation sets as proposed in the *lmms-eval* [123] when available for the captioning and VQA tasks. We use the full evaluation set for MMMU and POPE. We leverage the full eval set for RefCOCO, RefCOCO+, and RefCOCog experiments.

**General Results** Overall, on the 10 datasets and 6 tasks and 11 sub-tasks considered (Fig. 6 and Tab. 1), we achieve large improvement for captioning, referring, hallucination control and object recall; and comparable or better performance for multitasking benchmarks and VQA, obtaining almost 20% improvement for the best performing one (captioning) and around 1% decrease in performance for the worst performing tasks (visual question answering). For referring tasks, we can see that for a VLM with poor refer-

ring capacity (LLaVA-1.6-7b w/ Mistral), leveraging SVP increases the model performance on referring generation three folds.

**Captioning Tasks** In Fig. 7 we explore captioning for a 13b language architecture (Vicuna) over 3 datasets (COCO2017, Flickr30k, NoCaps). In Appendix Tab. 6 we consider fine-grained metrics for captioning over four datasets (COCO2017, Flickr30k, NoCaps, and RefCOCO). In Appendix Tab. 9 the models are assessed using different feedback mechanisms: no feedback (baseline sampling from  $p_\theta(\mathbf{z}|\mathbf{c})$ ), and with feedback for the first SVP iteration, sampling  $q_1(\mathbf{z}|\mathbf{c}, \mathbf{g})$ , and the second, sampling  $q_2(\mathbf{z}|\mathbf{c}, \mathbf{g})$ . We also evaluate performance with visual queries (VQ). SVP consistently outperforms other methods across all evaluated datasets. This finding highlights the impact of integrating sampling and feedback mechanisms in enhancing the model’s image captioning abilities. These results support our hypothesis that improving visual-language alignment is a fundamental principle for advancing the capabilities of VLMs.

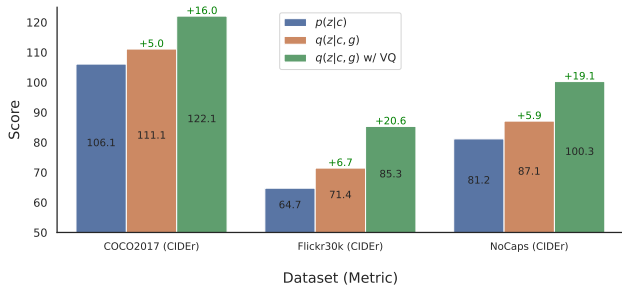


Figure 7. **Captioning Performance** of LLaVA-1.6-13b model. This table compares the image captioning capabilities of the LLaVA-1.6-13b model (featuring CLIP vision encoder and Vicuna language model) across various sampling methods. We evaluate performance when sampling from the prior (without feedback) and the posterior (with feedback). The analysis ablates different feedback mechanisms: 1) sampling from the prior  $p(\mathbf{z}|\mathbf{c})$  (no feedback), 2) sampling from the posterior  $q(\mathbf{z}|\mathbf{c}, \mathbf{g})$  (with feedback), and 3) incorporating visual queries (w/ VQ). CIDEr scores are reported for each dataset, quantifying captioning quality. For comprehensive results across model sizes and architectures, see Appendix Tab. 9.

**Referring Tasks** In Fig. 8 and Appendix Tab. 12 we study model performance for referring-based tasks, where the VLM is tasked with describing a specific region. We compare the performance of different models, including a base model, a model tuned without grounding (w/o  $\mathbf{g}$ ), a model tuned with visual grounding (w/ SVP (C)), and a model with SVP and visual queries (w/ SVP (CVQ)). The results show significant performance improvements leveraging SVP across datasets and tasks. SVP significantly improves the

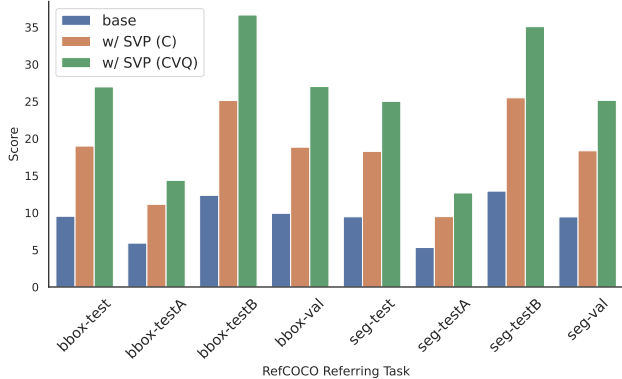


Figure 8. **Referring Expression Generation Performance** on RefCOCO Tasks. Comparison of LLaVA-1.6-7b variants: base model, SVP, and SVP with VQ. We report CIDEr scores for detection (bbox) and segmentation (seg) tasks on test and validation sets. SVP significantly outperforms the base model, demonstrating the effectiveness of visual grounding as feedback. SVP models are adapted without access to bounding boxes. See Appendix Tab. 12 for RefCOCO+ and RefCOCOg experiments.

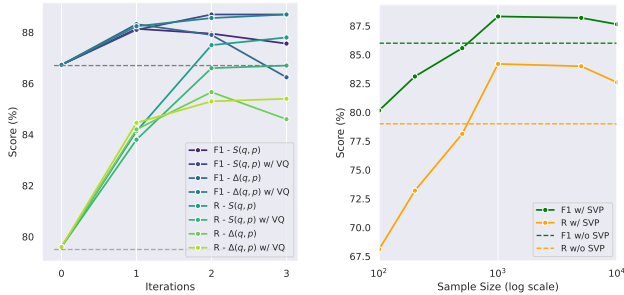
base model’s referring and spatial understanding abilities, especially when initial performance is low, reaching close to parity with a larger 13b model (Tab. 1). Notably, this enhancement occurs without direct access to grounding information (bounding boxes) during adaptation; grounding conditioning  $\mathbf{g}$  is only used in the inner-loop sampling to build  $q(\mathbf{z}|\mathbf{c}, \mathbf{g})$  (Fig. 2.(iii)). Afterward, we fine-tune model parameters  $\theta$  using the refined visual projections  $\mathbf{z}$ . The success of SVP in improving referring abilities without direct grounding information indicates that modality alignment is central to spatial understanding in VLMs.

**Hallucination and Object Recall** In Tab. 2 and Appendix Tab. 11 we provide evaluation for hallucination rate in our model. In Fig. 6 and Fig. 9a we also consider object recall as a measure of how much of the visual input is missing in the textual output. SVP provides a significant performance boost for most of the considered model variants (Tab. 2) on the POPE dataset. For the 7B model, adding SVP increases the overall F1 score from 86.7% to 88.3%, performing on par with models five times larger (Appendix D.5). For the 13B model, SVP improves the overall score from 86.2% to 87.5%. Fig. 9a demonstrates that running SVP for  $I = 3$  iterations, coupled with the scoring mechanism outlined in Eq. (3), significantly enhances object recall from approximately 79% to over 87%. These findings offer compelling evidence that improved modality alignment, achieved through self-captioning and grounding feedback, effectively mitigates hallucinations without the need for specialized fine-tuning aimed at hallucination reduction, corroborating our underlying hypothesis. SVP substantially augments the

Model	$v_{\theta}$	$t_{\theta}$	Adaptation	ScienceQA	VQA	GQA	NoCaps	Captioning	Flickr30k	Referring	Multitasking	Hallucinations		
				test	VQAv2 val_lite	lite	val_lite	COCO2017 val_lite	test_lite	RefCOCO-bbox val_lite	MMBench en_dev_lite	MMMU val	POPE (F1) all	POPE (R) all
LLaVA-1.6-7b	CLIP	Mistral	-	<b>78.54</b>	<b>76.68</b>	<b>75.80</b>	92.60	109.68	78.74	6.70	<b>80.30</b>	34.11	86.73	79.60
LLaVA-1.6-7b	CLIP	Mistral	SVP (C)	77.24	74.98	73.80	100.93	112.95	83.49	18.15	77.27	36.44	<b>88.33</b>	<b>84.20</b>
LLaVA-1.6-7b	CLIP	Mistral	SVP (CVQ)	<b>78.40</b>	75.18	<b>75.10</b>	<b>103.95</b>	<b>115.02</b>	<b>85.31</b>	<b>24.74</b>	78.03	<b>37.44</b>	<b>88.25</b>	<b>84.41</b>
				↓ 0.97 %			↑ 8.48 %		↑ 18.04	↑ 3.43 %		↑ 3.94 %		
LLaVA-1.6-13b	CLIP	Vicuna	-	70.30	<b>77.26</b>	<b>74.60</b>	83.89	104.21	69.86	<b>29.71</b>	<b>83.33</b>	35.22	86.24	78.13
LLaVA-1.6-13b	CLIP	Vicuna	SVP (C)	<b>74.34</b>	76.60	<b>74.40</b>	87.09	111.09	71.43	28.93	81.06	<b>36.33</b>	<b>87.44</b>	81.20
LLaVA-1.6-13b	CLIP	Vicuna	SVP (CVQ)	68.49	76.26	73.20	<b>100.26</b>	<b>122.03</b>	<b>85.32</b>	27.20	78.03	35.66	<b>87.68</b>	<b>82.53</b>
				↑ 1.58 %			↑ 19.58 %		↓ 0.78	↑ 0.12 %		↑ 3.65 %		

Table 1. **Benchmark Performance** of LLaVA variants on vision-language tasks. We utilize the `lmms-eval` library with the `lite` split as proposed by [123], employing full evaluation sets for MMMU and POPE. The table presents results for various LLaVA model configurations, encompassing different model sizes (7B and 13B), visual and text encoders (CLIP and Mistral/Vicuna), and adaptation techniques (SVP and SVP with VQ). A single iteration of SVP is applied across all experiments. Higher scores indicate better performance for all metrics. Our findings demonstrate that SVP enhances performance on captioning and referring tasks, reduces hallucinations, and improves object recall, while maintaining strong results on multitask benchmarks and visual question answering. This comprehensive evaluation underscores the efficacy of our proposed method across diverse vision-language challenges. More results in Appendix Tab. 13.

model’s ability to deliver accurate, factual information.



(a) Results with  $C = 1000$  for  $I = 3$  iterations with entropy-based  $\Delta(q, p)$  and kl-based  $S(q, p)$  scores. Higher is better. (b) Results with  $I = 1$  a single iteration increasing the sample size  $C \in (0.1, 0.2, 0.5, 1, 5, 10)k$ . Higher is better.

Figure 9. **Iteration and Sample Size Ablation.** We ablate the number of iterations  $I$  and sample size  $C$  for hallucination rate (F1) and object recall (R) using LLaVA-1.6-7b and SVP. Higher is better.

**Ablations** In Tab. 3 we ablate the different components of SVP (grounding, scoring, VQ). In Fig. 9a, Appendix Fig. 15, and Tab. 9 we analyze the effect of the number of iterations  $I$ , and in Fig. 9b how SVP behaves increasing the sample size  $C$ . In Tab. 13 we ablate entropy-based  $\Delta(q, p)$  and divergence-based  $S(q, p)$ , scores on the full benchmark. In table Tab. 4 and Tab. 14 we compare SVP with DPO and preference-alignment.

## 5. Conclusions

**Limitations** SVP requires a VLM capable of in-context learning and multiple samples per input. Its effectiveness is limited by the underlying grounding model’s quality and may not improve tasks without spatial understanding or those requiring specialized knowledge. Future work could explore

Model	Size	$v_{\theta}$	$t_{\theta}$	POPE (F1 score $\uparrow$ )			
				adv	pop	random	all
LLaVA [62]	7b	CLIP	Vicuna	72.0	75.3	80.7	76.0
LLaVA-SFT+ [93]	7b	CLIP	Vicuna	80.1	82.4	85.5	82.7
LLaVA-RLHF [93]	7b	CLIP	Vicuna	79.5	81.8	83.3	81.5
LLaVA [62]	13b	CLIP	Vicuna	74.4	78.2	78.8	77.1
LLaVA-SFT+ [93]	13b	CLIP	Vicuna	81.1	82.6	84.8	82.8
LLaVA-RLHF [93]	13b	CLIP	Vicuna	80.5	81.8	83.5	81.9
LLaVA-NeXT-DPO [61]	7b	CLIP	Qwen2	83.43	83.78	84.73	83.98
LLaVA-OV-DPO [52]	7b	SigLIP	Qwen2	85.12	86.24	87.37	86.24
LLaVA-HA-DPO [124]	7b	CLIP	Vicuna	82.54	<b>87.89</b>	<b>90.25</b>	86.90
LLaVA-1.5 [60]	13b	CLIP	Vicuna	84.53	86.31	87.17	86.00
LLaVA-1.5 w/ SVP	13b	CLIP	Vicuna	84.66	86.84	87.44	86.31
LLaVA-1.6 [61]	7b	CLIP	Mistral	<b>85.43</b>	86.87	88.05	86.73
LLaVA-1.6 w/ SVP	7b	CLIP	Mistral	<b>85.93</b>	<b>89.04</b>	<b>90.02</b>	<b>88.33</b>
LLaVA-1.6 [61]	13b	CLIP	Vicuna	85.17	86.36	87.20	86.24
LLaVA-1.6 w/ SVP	13b	CLIP	Vicuna	85.15	87.50	89.23	<b>87.30</b>
LLaVA-OV [52]	0.5b	SigLIP	Qwen2	82.28	83.19	83.89	83.12
LLaVA-OV w/ SVP	0.5b	SigLIP	Qwen2	83.45	84.70	85.46	84.53
<i>Bigger VLMs</i>							
LLaVA-1.6 [61]	34b	CLIP	Yi-2	-	-	-	87.7
InternVL-1.2 [18]	40b	IVIIT	Yi-2	-	-	-	88.0
InternVL-1.2+ [18]	40b	IVIIT	Yi-2	-	-	-	88.7
VILA-1.5 [58]	40b	IVIIT	Yi2	-	-	-	87.3
VILA-1.5-AWQ [58]	40b	IVIIT	Yi2	-	-	-	88.2

Table 2. **Hallucination Mitigation** performance on POPE benchmark. Comparison of LLaVA model variants’ F1 scores across adversarial, popular, random, and overall splits. Results demonstrate impacts of model size, fine-tuning strategy, encoder choices, and SVP adaptation on hallucination avoidance. See Appendix Tab. 11 and Appendix D.5 for extended results.

augmentation and guided-search strategies to enhance localized visual input processing.

In this work, we introduced SVP, a novel approach that elicits latent information in VLMs through self-captioning and grounding as a feedback mechanism, without requiring additional annotations. SVP is effective in enhancing captioning quality, referring expression generation, hallucination control, and object recall, while maintaining competitive performance in VQA and multitasking. These results underscore the potential of SVP to unlock latent capabilities in



Model	Grounding	Scoring	VQ	RefCOCO	Flickr30k	MMMU	POPE
LLaVA	-	-	-	6.70	78.74	34.11	86.73
LLaVA w/o SVP	✗	✗	✗	3.01	79.03	35.55	87.21
LLaVA w/ SVP	✓	✗	✗	9.98	78.67	35.77	86.92
LLaVA w/ SVP	✓	✓	✗	18.15	83.49	36.44	<b>88.33</b>
LLaVA w/ SVP	✓	✓	✓	<b>24.74</b>	<b>85.31</b>	<b>37.44</b>	88.25

Table 3. **Component Ablation.** Performance comparison of LLaVA-1.6-7b variants after one adaptation iteration: base model, fine-tuning without feedback, sampling with grounding (no scoring), grounding with scoring, and full SVP (grounding, scoring, visual queries). Results provide evidence of the importance of the SVP’s components for model performance.

Model	Samples	SciQA	NoCaps	RefCOCO	MMBench	POPE
w/ DPO	$\geq 9.4k$	79.25	112.51	13.60	85.60	86.24
w/ SVP (C)	$\approx 2k$	83.89	120.23	15.75	86.36	85.78

Table 4. **Preference Ablation.** Comparison between SVP and DPO [78] for LLaVA-7b-OV. Higher is better. DPO relies on a learned reward model for annotation or a labelled set of positive/negative pairs following human preferences. SVP relies on a small grounding model as feedback. We set  $C = 2000$ ,  $K = 10$ , and select the top 10%. Preference optimization is typically used to improve alignment between model output and a set of preferences. However, preference alignment does not correspond to better visual language alignment compared to SVP.

VLMs efficiently, paving the way for more robust and accessible vision-language models with real-world applications. Our findings highlight the importance of visual-language alignment and the power of self-improvement techniques in advancing multimodal AI systems, reducing the need for extensive training data and computational resources.

# **Supervision-free Vision-Language Alignment**

## *Supplementary Material*

**Instruction:** Please describe the content of this image as detailed as possible.

**VLM response:**  
 The image depicts a modern home office setup. At the center of the scene is a wooden desk with a sleek, minimalist design. The desk features a flat surface with a built-in drawer and a small shelf on the left side. **On the right side of the desk, there is a laptop open and ready for use.** Above the desk, mounted on the wall, is a framed artwork of a ballerina in a dynamic pose, adding a touch of elegance and movement to the space. The artwork is encased in a black frame that contrasts with the wall's dark gray color. **To the left of the desk, there is a floor lamp with a modern design, providing additional lighting.** The lamp has a tall, slender base and a curved arm with a white shade. On the desk, there is a small plant in a white pot, adding a touch of greenery and life to the space. The plant is placed on the left side of the desk, near the laptop. Underneath the desk, there is a black wire basket, which is likely used for cable management and storage.

**Note:** missing chair, missing background.

**Grounded Objects:** desk (0.82). laptop (0.93). artwork (0.64). frame (0.74). lamp (0.87). plant (0.83). pot (0.68). basket (0.83).

**Instruction:** Please describe the content of this image as detailed as possible.  
**Context:** Use the following context. The list of numbers are bounding boxes for the objects. Check if object and bounding boxes connections are correct. Check if there are additional objects in the image and describe them.  
**format:** cxcywh.  
**boxes:** lamp [0.33,0.47,0.16,0.23], laptop [0.48,0.54,0.16,0.09], desk [0.49,0.75,0.61,0.33], plant [0.36,0.56,0.04,0.06], frame [0.64,0.22,0.24,0.24], basket [0.80,0.80,0.15,0.15].

**VLM response:**  
 The image depicts a modern workspace setup against a dark gray wall with horizontal wood paneling. On the wall, there is a framed artwork featuring a figure in a red dress with a blue background, possibly a painting or a print. Below the artwork, there is a desk with a light wood finish. The desk has a rectangular shape with a flat top and is supported by four black metal legs. **On the desk, there is a laptop with a black screen and a silver body, positioned towards the center.** To the left of the laptop, there is a white desk lamp with a curved neck and a silver base, turned off. Next to the lamp, there is a small white potted plant with green leaves. In front of the desk, there is a white office chair with a modern design, featuring a curved backrest and armrests. The chair is positioned facing the desk, with the seat slightly pulled out. To the right of the desk, there is a black wire basket with a handle, placed on the floor. The flooring appears to be a light-colored wooden plank. The overall lighting in the room is soft and ambient, suggesting a calm and focused work environment.

**Grounded Objects:** artwork (0.83). desk (0.85). laptop (0.94). desk lamp (0.84). potted plant (0.83). office chair (0.90). wire basket (0.94). flooring (0.64).

Figure 10. **Sampling VLMs with and without Grounding Feedback.** Incorporating grounding feedback helps VLMs to focus on factual information and better describe the details in the input image. We use GroundingDINO [63], an open-set grounding model, to obtain the conditioning information. When the predicted bounding boxes overlap above a certain threshold, we select the box with the highest score, following a standard non-maximum-suppression approach. By leveraging this grounding feedback, the model is better able to specify the entities and relationships between the objects in the image, leading to an improved parsing of the visual information. This results in more accurate and detailed descriptions, such as identifying a desk lamp instead of a floor lamp, mentioning an office chair, describing the flooring in the background, and differentiating between an artwork and a simple frame, or a potted plant and a generic plant. More visualizations in Appendix I.

## A. Qualitative Text-to-Image Generation

Model	Size	ITMScore (BLIP2)	ImageReward
LLaVA-1.6	7b	0.83	0.47
LLaVA-1.6 w/ SVP	7b	<b>0.88</b>	<b>0.49</b>
LLaVA-1.6	13b	0.82	0.44
LLaVA-1.6 w/ SVP	13b	<b>0.87</b>	<b>0.45</b>

Table 5. Text-to-Image alignment scores computed using base VLMs and VLMs adapted with SVP. Image Text Matching (ITM [54]) and ImageReward [108] are traditionally used to evaluate AI-generated images from real text prompts. Here we apply these scores to assess AI-generated captions for real images. Although Text-to-Image alignment is not fully indicative of Image-to-Text alignment in this context, these scores provide an additional qualitative measure of caption-image correspondence. Higher is better.



(a) Input image



(b) Text-to-Image generation using base VLM response -  $\mathbf{z} \sim p_{\theta}(\mathbf{z}|\mathbf{c})$ . See left side Fig. 10.



(c) Text-to-Image generation using grounded VLM response -  $\mathbf{z} \sim q(\mathbf{z}|\mathbf{c}, \mathbf{g})$ . See right side Fig. 10.

Figure 11. FLUX-schnell [50] text to image generation using the original VLM response (left) and the response leveraging grounding (right) as input. For each approach, we generated a single image without multiple attempts or selective filtering. The comparison clearly illustrates that the grounding-enhanced response produces more accurate and reliable generation outcomes.



(a) Input image from coco2017\_cap\_val\_lite. Image id: 000000466567. Target Captions (provided as ground truth): ["A tree with a donut as an ornament", "A plastic tree with a doughnut hanging by a strip of red ribbon. ", "A Christmas ornament is a donut with a squirrel on it.", "A doughnut hanging from a Christmas tree as a decoration.", "a donut being used as an ornament for a christmas tree"]



(b) Text-to-Image generation using base VLM response: "A donut with a red ribbon and a small toy animal on it" for image (a).



(c) Text-to-Image generation using VLM w/ SVP response: "A donut with a red ribbon and a small toy animal on a Christmas tree" for image (a).

Figure 12. FLUX-schnell [50] text to image generation using the base VLM response (left) and the response using SVP (right) as input. We generated a single image without multiple attempts or selective filtering.



(a) Input image from `coco2017_cap_val_lite`. Image id: 000000253742. Target Captions (provided as ground truth): ["A woman standing next to a herd of animals.", "a woman holding an umbrella at the park", "A woman standing in the rain with an umbrella with a herd of deer behind her.", "On a rainy day at the zoo umbrellas are frequently seen.", "Several people holding umbrellas and standing next to deer."]



(b) Text-to-Image generation using base VLM response: "A group of people holding umbrellas and standing in the rain" for image (a).



(c) Text-to-Image generation using VLM w/ SVP response: "A woman holding an umbrella stands among a group of people and deer" for image (a).

Figure 13. FLUX-schnell [50] text to image generation using the base VLM response (left) and the response using SVP (right) as input. We generated a single image without multiple attempts or selective filtering.

## B. SVP Algorithm

---

### Algorithm 1 Supervision-free Vision-Language Projection (SVP)

---

**Require:**  $\mathbf{c} = (\mathbf{c}_t, \mathbf{c}_v)$ : input prompts,  $\mathbf{c}_t$ : input text,  $\mathbf{c}_v$ : input image,  $S$ : scoring function,  $p_\theta$ : base VLM,  $q$ : grounded VLM,  $g$ : grounding model,  $I$ : number of outer-loop iterations,  $C$ : number of inner-loop input prompts,  $T$ : sequence length.

**Ensure:**  $i = 0$  ▷ set outer – loop iterator

**Ensure:**  $\theta_0 \leftarrow \theta$  ▷ set base model as initialization

**while**  $i < I$  **do** ▷  $i_{th}$  iteration

**for**  $c = 1 : C$  **do** ▷ inner – loop - sampling

    Sample  $\mathbf{z} \sim p_{\theta_i}(\mathbf{z}|\mathbf{c})$  ▷ sample  $i_{th}$  model

$\mathbf{g} \leftarrow g(\mathbf{z}, \mathbf{c}_v)$  ▷ run grounding

$\{\mathbf{z}_g\}_K \sim q(\mathbf{z}|\mathbf{c}, \mathbf{g})$  ▷  $K$  posterior samples

$\{s\}_K \leftarrow S(q, p_{\theta_i}, \{\mathbf{z}_g\}_K)$  ▷ score samples

$x_k \leftarrow \text{argsort} \{s\}_K$  ▷ sort indexes

$\mathbf{z}_g^k \leftarrow \mathbf{z}_g[x_k]$  ▷ select top  $k$  samples

**end for**

$\mathcal{L}(\theta) \leftarrow \text{outer – loop}(\{\mathbf{z}_g^k, \mathbf{c}\}|_C, p_\theta)$  ▷ loss for  $i_{th}$  iteration

$\theta_i \leftarrow \theta - \nabla_\theta \mathcal{L}(\theta)$  ▷ adapt base model

$i \leftarrow i + 1$  ▷ update iteration

**end while**

$\theta_g \leftarrow \theta_I$

$\mathbf{z}_g \sim p_{\theta_g}(\mathbf{z}|\mathbf{c})$  ▷ adapted model

---

## C. Extended Related Work

**Improving Vision-Language Models** Researchers have investigated explicit grounding in VLMs, primarily to address hallucinations [26, 102], with less focus on developing general paradigms for improving vision-language alignment. A common strategy involves incorporating grounding annotations into training data [73] for vision-centric VLMs [11, 113, 115, 122]. However, this annotation process is costly, time-consuming, and prone to errors. For instance, directly generating coordinate tokens as output is sample-inefficient, requiring billions of annotations even for small VLMs to develop a competitive detector [115]. While explicit supervision during fine-tuning can enhance alignment between visual and linguistic representations [60, 93], these train-time methods necessitate large amounts of high-quality visual-text data and are resource-intensive to scale with human annotations. Train-time techniques like Reinforcement Learning from Human Feedback (RLHF [20, 69]) and Direct Preference Optimization (DPO [78]), primarily used for aligning LLMs with human preferences, can be adapted to align VLM text outputs with visual inputs [93, 104, 125]. These approaches incorporate feedback and preferences during post-training but are limited by the need for reward signals [93], curated preference pairs [125, 127], and AI feedback [104]. Test-time methods [102], such as Visual Contrastive Decoding [51] and Multi-Modal Mutual-Information Decoding [26], aim to improve grounding at inference by leveraging differences between vision-conditional and unconditional models, without altering the model architecture or training. Woodpecker [112] proposes a five-step inference procedure to mitigate hallucination. While somewhat effective, these methods often require memory-intensive and computationally expensive inference, as well as model-specific heuristics, which limits their generalization and usability.

**Grounding in Vision-Language Models** Visual grounding can be conceptualized as the dual of text-image alignment. When viewed as a mechanism to elicit and organize information within Vision-Language Models (VLMs), it represents a form of alignment between visual and textual modalities, encompassing both representation and generation aspects. The concept of grounding has deep roots in cognitive sciences [4, 9, 29, 47]. In the context of computer vision, visual grounding can be seen as an extension of the classic closed-set detection problem [16, 28, 80, 121]. Traditional object detection tasks involve regressing bounding box coordinates and assigning class labels to regions within an input image. While leveraging curated benchmark datasets [59] has led to rapid improvements in precision and speed, this approach has been constrained by predefined class sets. Scaling to a larger number of classes and adapting to varying detection granularities have proven challenging [23, 33]. Visual grounding inverts this paradigm by using the set of classes as input and employing a vision-language model to assign bounding boxes to each element in the input. This concept can be further generalized to accommodate captions, descriptions, and various forms of textual input. Contrastive models such as GLIP [55] and GroundingDINO [63] offer flexible, generalized detection models that enhance spatial understanding [112] and serve as foundations for a wide range of tasks. Moreover, auto-regressive VLMs have been developed to perform grounding and referring tasks [73, 97, 113, 115], further expanding the capabilities of these models in bridging visual and linguistic information.

**Self-improvement in Vision and Language Models** Self-improving autonomous learners have been a long standing goal of the AI field [84, 85]. In the context of Vision-Language Models (VLMs), self-improvement can be conceptualized as a form of self-play [89, 90], where the model enhances its performance through sampling and external feedback mechanisms [5]. The advent of Large Language Models (LLMs) [1, 14] has necessitated novel approaches to self-improvement, given the challenges in defining explicit feedback for natural language trajectories. Notably, Reinforcement Learning from Human Feedback (RLHF) [69] and Reinforcement Learning from AI Feedback (RLAIF) [6] have emerged as prominent mechanisms. These methods score samples from the base model and select preferred outputs based on specific criteria, such as human preferences in chat interactions. Both approaches learn preference or reward models from human or AI feedback, and these concepts have been successfully adapted to VLMs [26, 93]. Further developments in this field include using rewards for ranking [24] and implicitly specifying preferences through positive and negative pairs [78]. Alignment can also be achieved through AI distillation [19, 92] and self-refinement techniques [44, 45, 94, 103]. A recent class of algorithms for self-improvement involves iterative processes [5, 32, 117, 118] that leverage feedback to enhance downstream tasks and reasoning chains [105] in LLMs. Moreover, feedback can be incorporated at inference time [65] and even utilize the model’s own capabilities as evaluator [88, 110]. These methods can be seen as instantiating meta-learning algorithms. Meta-learning [27, 38, 83], often described as learning to learn, plays a crucial role in the development of self-improving AI systems. This approach aims to create models that can adapt quickly to new tasks by leveraging knowledge from previously learned tasks [84, 85]. In the context of VLMs and LLMs, meta-learning techniques have been explored to enhance model adaptability and generalization across diverse domains. For instance, few-shot in-context learning methods [3, 14, 107] demonstrate how large models can rapidly adapt to new tasks with minimal task-specific examples.



## D. Additional Experiments

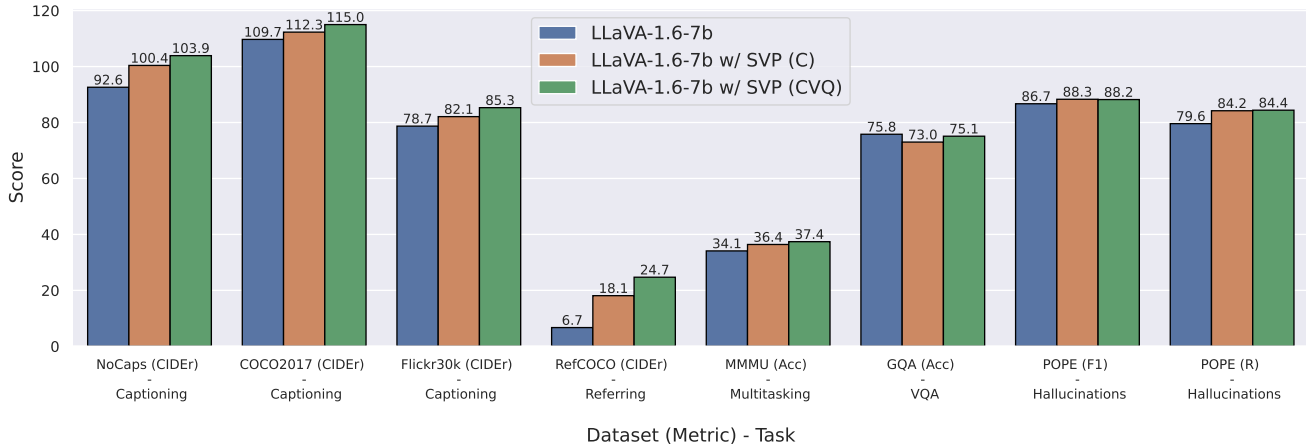


Figure 14. **Benchmark Results for Captioning, Referring, VQA, Multitasking, Hallucination control, and Object Recall** for a base VLM (LLaVA-16.7b) and the same VLM adapted using our method *SVP*. Higher is better for all the tasks, datasets, and metrics. The VLM demonstrates improved performance across key tasks like image captioning, referring expression comprehension, and hallucination control when adapted using the *SVP* technique. The model was adapted on 1000 COCO2014 images, using self-captioning and GroundingDINO as feedback signals. While captioning and referring saw clear gains, multitasking and VQA remained largely stable. Notably, there was a significant reduction in hallucinations compared to the base model. These results provide evidence that grounding as feedback can be leveraged to elicit latent knowledge in the model and improve visual-language alignment.

### D.1. Captioning

		BLEU-4	BLEU-3	BLEU-2	BLEU-1	METEOR	ROUGE-L	CIDEr
COCO2017	-	0.31	0.41	0.54	0.68	0.26	0.54	1.09
	w/ <i>SVP</i>	0.34	0.45	0.60	0.77	0.28	0.57	1.15
Flickr30k	-	0.29	0.39	0.53	0.70	0.23	0.51	0.78
	w/ <i>SVP</i>	0.29	0.41	0.56	0.74	0.24	0.51	0.82
NoCaps	-	0.37	0.49	0.62	0.76	0.26	0.54	0.92
	w/ <i>SVP</i>	0.39	0.52	0.67	0.82	0.28	0.57	1.01
RefCOCO	-	0.01	0.01	0.01	0.03	0.06	0.09	0.06
	w/ <i>SVP</i>	0.01	0.01	0.02	0.04	0.07	0.13	0.18

Table 6. Comparison of various evaluation metrics for image captioning models with and without the *SVP* technique across different datasets in the `lmms-eval-lite` benchmark [123]. This table presents the performance of image captioning models on several standard evaluation metrics, including BLEU, METEOR, ROUGE-L, and CIDEr. The models are evaluated on the COCO, Flickr30k, NoCaps, and RefCOCO datasets, both with and without the use of *SVP*. The results provide a comprehensive overview of the impact of the *SVP* approach on the captioning quality across different datasets and metrics.

	Score	COCO2014_val			COCO2017_val			NoCaps_test			Flickr30k_test		
		M	R	C	M	R	C	M	R	C	M	R	C
LLaVA-1.6-7b	-	26.14	54.25	107.65	26.00	54.12	109.32	27.03	56.98	96.08	23.63	51.61	73.17
LLaVA-1.6-7b w/ SVP (C)	$\Delta(q, p)$	28.74	56.69	111.98	28.74	56.69	114.77	29.37	59.52	104.79	25.62	53.25	75.98
LLaVA-1.6-7b w/ SVP (CVQ)	$\Delta(q, p)$	29.26	56.62	111.38	29.24	56.67	114.72	30.07	59.69	104.58	26.34	53.58	77.68
LLaVA-1.6-7b w/ SVP (C)	$S(q, p)$	28.64	56.74	112.45	28.57	56.71	114.69	29.29	59.62	104.75	25.54	53.40	76.53
LLaVA-1.6-7b w/ SVP (CVQ)	$S(q, p)$	29.22	56.25	109.57	29.25	56.34	113.08	30.08	59.55	104.01	26.26	53.23	76.73
LLaVA-1.6-13b	-	24.67	52.03	99.39	24.72	52.23	102.04	25.44	54.93	88.13	22.21	48.78	66.68
LLaVA-1.6-13b w/ SVP (C)	$\Delta(q, p)$	25.31	54.28	104.83	25.30	54.40	107.20	26.16	57.21	93.11	22.54	50.82	67.77
LLaVA-1.6-13b w/ SVP (CVQ)	$\Delta(q, p)$	28.38	56.71	113.30	28.49	57.03	117.23	28.94	59.19	102.32	25.69	53.61	78.11
LLaVA-1.6-13b w/ SVP (C)	$S(q, p)$	25.32	54.22	104.84	25.37	54.37	107.52	26.14	57.14	93.11	22.71	51.00	68.56
LLaVA-1.6-13b w/ SVP (CVQ)	$S(q, p)$	28.39	56.54	112.65	28.35	56.67	116.09	28.96	59.14	101.93	25.59	53.25	77.00

Table 7. Captioning Performance for the full benchmark datasets using `lmms-eval` [123]. We use the full evaluation sets (around 80k samples) instead of only considering the `lite` versions. See Appendix J for dataset details.  $\Delta(q, p)$  represents a scoring mechanism based on the differential between entropy.  $S(q, p)$  represents a scoring mechanism based on the log-ratio output distribution for a VLM w/ and w/o grounding. The table compares the results of different LLaVA model configurations, with varying model sizes (7B and 13B). We consider NoCaps, COCO2017, Flickr30k for captioning. We use METEOR (M), ROUGE-L (R), CIDEr (C) scores for captioning tasks. Higher is better for all the metrics.

	Score	COCO2014_val				COCO2017_val				NoCaps_test			Flickr30k_test				
		B4	B3	B2	B1	B4	B3	B2	B1	B4	B3	B2	B1	B4	B3	B2	B1
LLaVA-1.6-7b	-	31.04	41.51	54.40	68.81	30.82	41.24	54.14	68.54	38.43	50.03	62.89	75.43	28.57	39.90	54.54	71.41
LLaVA-1.6-7b w/ SVP (C)	$\Delta(q, p)$	32.29	44.25	59.33	76.16	32.61	44.50	59.44	76.09	41.05	54.12	68.82	83.18	28.94	40.62	55.85	73.53
LLaVA-1.6-7b w/ SVP (CVQ)	$\Delta(q, p)$	31.69	43.50	58.46	75.52	32.01	43.72	58.53	75.53	40.88	53.78	68.49	83.42	29.22	40.71	55.63	73.27
LLaVA-1.6-7b w/ SVP (C)	$S(q, p)$	32.75	44.76	59.86	76.71	32.82	44.74	59.78	76.54	41.15	54.17	68.77	82.93	29.59	41.38	56.68	74.36
LLaVA-1.6-7b w/ SVP (CVQ)	$S(q, p)$	30.95	42.67	57.60	74.76	31.46	43.02	57.78	74.86	40.29	53.27	68.16	83.17	28.76	40.09	54.90	72.56
LLaVA-1.6-13b	-	27.33	36.76	48.51	61.98	27.64	37.06	48.84	62.33	34.06	44.86	56.93	68.78	24.28	34.50	48.31	65.26
LLaVA-1.6-13b w/ SVP (C)	$\Delta(q, p)$	29.97	39.65	51.34	63.79	29.96	39.65	51.37	63.76	37.28	48.33	59.97	70.31	27.15	37.88	51.83	67.78
LLaVA-1.6-13b w/ SVP (CVQ)	$\Delta(q, p)$	33.65	45.40	59.99	76.45	34.28	45.90	60.43	76.71	40.77	53.66	68.09	82.25	29.91	41.92	57.53	75.55
LLaVA-1.6-13b w/ SVP (C)	$S(q, p)$	29.97	39.78	51.67	64.45	30.25	39.97	51.83	64.56	37.54	48.61	60.40	71.12	27.60	38.64	52.60	68.83
LLaVA-1.6-13b w/ SVP (CVQ)	$S(q, p)$	33.45	45.26	59.90	76.47	34.00	45.59	60.10	76.50	40.35	53.24	67.81	82.17	29.40	41.39	57.03	75.18

Table 8. Captioning Performance for the full benchmark datasets using `lmms-eval` [123]. We use the full evaluation sets (around 80k samples) instead of only considering the `lite` versions. See Appendix J for dataset details.  $\Delta(q, p)$  represents a scoring mechanism based on the differential between entropy.  $S(q, p)$  represents a scoring mechanism based on the log-ratio output distribution for a VLM w/ and w/o grounding. The table compares the results of different LLaVA model configurations, with varying model sizes (7B and 13B). We consider NoCaps, COCO2017, Flickr30k for captioning. We use BLEU-4 (B4), BLEU-3 (B3), BLEU-2 (B2), BLEU-4 (B1) scores for captioning tasks. Higher is better for all the metrics.

Model	Size	$v_\theta$	$t_\theta$	Feedback	COCO2017	Flickr30k	NoCaps	TextCaps
LLaVA-1.6	13b	CLIP	Vicuna	-	104.21	69.86	83.89	69.91
LLaVA-1.6	13b	CLIP	Vicuna	$p_\theta(\mathbf{z} \mathbf{c})$	106.08	64.74	81.16	57.10
LLaVA-1.6	13b	CLIP	Vicuna	$q_1(\mathbf{z} \mathbf{c}, \mathbf{g})$	110.19	71.44	87.09	59.09
LLaVA-1.6	13b	CLIP	Vicuna	$q_1(\mathbf{z} \mathbf{c}, \mathbf{g})$ w/ VQ	119.15	<b>85.32</b>	<b>100.26</b>	<b>71.57</b>
LLaVA-1.6	13b	CLIP	Vicuna	$q_2(\mathbf{z} \mathbf{c}, \mathbf{g})$ w/ VQ	<b>123.24</b>	82.45	99.43	66.20

Table 9. Performance of the LLaVA-1.6-13b model on various captioning datasets using the `lmms-eval-lite` benchmark [123]. The table ablates the feedback mechanisms employed, such as sampling from the prior (no feedback,  $p(\mathbf{z}|\mathbf{c})$ ), sampling from the posterior (with feedback,  $q_1(\mathbf{z}|\mathbf{c}, \mathbf{g})$ ), sampling from the posterior iteratively (with feedback and two iterations,  $q_2(\mathbf{z}|\mathbf{c}, \mathbf{g})$ ), and with and without visual queries (VQ). We report the CIDEr score for each dataset, which evaluate the model’s image captioning capabilities.

Model	Size	$v_\theta$	$t_\theta$	POPE ( $F1$ score $\uparrow$ )			
				adv	pop	random	all
LLaVA [62]	7b	CLIP	Vicuna	72.0	75.3	80.7	76.0
LLaVA-SFT+ [93]	7b	CLIP	Vicuna	80.1	82.4	85.5	82.7
LLaVA-RLHF [93]	7b	CLIP	Vicuna	79.5	81.8	83.3	81.5
LLaVA [62]	13b	CLIP	Vicuna	74.4	78.2	78.8	77.1
LLaVA-SFT+ [93]	13b	CLIP	Vicuna	81.1	82.6	84.8	82.8
LLaVA-RLHF [93]	13b	CLIP	Vicuna	80.5	81.8	83.5	81.9
LLaVA-NeXT-DPO [61]	7b	CLIP	Qwen2	83.43	83.78	84.73	83.98
LLaVA-OV-DPO [52]	7b	SigLIP	Qwen2	85.12	86.24	87.37	86.24
LLaVA-HA-DPO [124]	7b	CLIP	Vicuna	82.54	<u>87.89</u>	<b>90.25</b>	86.90
LLaVA-1.5 [60]	13b	CLIP	Vicuna	84.53	86.31	87.17	86.00
LLaVA-1.5 w/ SVP	13b	CLIP	Vicuna	84.66	86.84	87.44	86.31
LLaVA-1.6 [61]	7b	CLIP	Mistral	<u>85.43</u>	86.87	88.05	86.73
LLaVA-1.6 w/ SVP	7b	CLIP	Mistral	<b>85.93</b>	<b>89.04</b>	<u>90.02</u>	<b>88.33</b>
LLaVA-1.6 [61]	13b	CLIP	Vicuna	85.17	86.36	87.20	86.24
LLaVA-1.6 w/ SVP	13b	CLIP	Vicuna	85.15	87.50	89.23	<u>87.30</u>
LLaVA-OV [52]	0.5b	SigLIP	Qwen2	82.28	83.19	83.89	83.12
LLaVA-OV w/ SVP	0.5b	SigLIP	Qwen2	83.45	84.70	85.46	84.53
LLaVA-1.6 [61]	34b	CLIP	Yi-2	-	-	-	87.7
InternVL [18]	19b	IViT	Vicuna	-	-	-	87.6
InternVL-1.2 [18]	40b	IViT	Yi-2	-	-	-	88.0
InternVL-1.2+ [18]	40b	IViT	Yi-2	-	-	-	88.7
VILA-1.5 [58]	8b	SigLIP	LLaMA3	-	-	-	85.6
VILA-1.5 [58]	8b	SigLIP	Vicuna	-	-	-	86.3
VILA-1.5 [58]	40b	IViT	Yi2	-	-	-	87.3
VILA-1.5-AWQ [58]	40b	IViT	Yi2	-	-	-	88.2

Table 10. Hallucination Mitigation performance on POPE benchmark. Comparison of LLaVA model variants’ F1 scores across adversarial, popular, random, and overall splits. Results demonstrate impacts of model size, fine-tuning strategy, encoder choices, and SVP adaptation on hallucination avoidance.

## D.2. Hallucination Rate

Model	Size	Eff-Size	$v_\theta$	$t_\theta$	POPE ( <i>Acc</i> score $\uparrow$ )		
					adv	pop	random
<i>Fine-tuning</i>							
InstructBLIP [22]	7b	7b	ViT	FlanT5	72.1	82.7	88.6
LLaVA-SFT <sup>+</sup> [93]	7b	7b	CLIP	Vicuna	80.2	82.9	86.1
mPLUG-Owl2 [111]	8b	8b	ViT	LLaMA2	84.1	86.2	88.3
InstructBLIP [22]	13b	13b	ViT	Vicuna	74.5	81.4	88.7
LLaVA-SFT <sup>+</sup> [93]	13b	13b	CLIP	Vicuna	82.3	83.9	85.2
<i>Test-time adaptation</i>							
QwenVL w/ VCD [51]	7b	14b	CLIP	Vicuna	84.3	87.1	88.6
LLaVA w/ M3ID [26]	7b	14b	CLIP	Vicuna	65.8	69.3	76.0
Otter w/ Woodpecker [112]	7b	$\geq 14b$	CLIP	LLaMA	83.0	84.3	86.7
mPLUG-Owl w/ Woodpecker [112]	7b	$\geq 14b$	ViT	LLaMA	81.0	84.1	86.3
LLaVA w/ M3ID [26]	13b	26b	CLIP	Vicuna	71.3	77.0	84.3
<i>Train-time adaptation</i>							
LLaVA-M3ID-DPO [26]	7b	7b	CLIP	Vicuna	68.2	73.9	81.2
LLaVA-RLHF [93]	7b	7b	CLIP	Vicuna	80.7	83.3	84.8
LLaVA-NeXT-DPO [78]	7b	7b	CLIP	Qwen2	85.2	85.6	86.6
LLaVA-OV-DPO [78]	7b	7b	SigLIP	Qwen2	86.3	87.5	88.7
LLaVA-HA-DPO [124]	7b	7b	CLIP	Vicuna	81.5	87.9	<b>90.5</b>
SeVa [127]	7b	7b	CLIP	Vicuna	83.6	87.4	89.4
LLaVA-M3ID-DPO [26]	13b	13b	CLIP	Vicuna	73.2	79.1	85.2
LLaVA-RLHF [93]	13b	13b	CLIP	Vicuna	82.3	83.9	85.2
InstructBLIP-HA-DPO [124]	13b	13b	ViT	Vicuna	80.7	85.8	89.8
LLaVA-1.6 [61]	7b	7b	CLIP	Mistral	86.4	87.9	89.2
LLaVA-1.6 w/ SVP	7b	7b	CLIP	Mistral	86.2	<b>89.6</b>	<b>90.6</b>
LLaVA-1.6 [61]	13b	13b	CLIP	Vicuna	86.4	87.7	88.5
LLaVA-1.6 w/ SVP	13b	13b	CLIP	Vicuna	<b>86.7</b>	88.4	89.2
LLaVA-OV	0.5b	0.5b	SigLIP	Qwen2	84.3	85.2	86.0
LLaVA-OV w/ SVP	0.5b	0.5b	SigLIP	Qwen2	85.0	86.3	87.2

Table 11. Evaluating hallucination rates in different VLMs adapted with fine-tuning, train-time adaptation, and test-time adaptation. Higher is better. Eff-Size: effective model size for multi-phase inference pipelines. Woodpecker [112] requires multiple models to process the response.

### D.3. Referring Tasks

			$\Delta(q, p)$		$S(q, p)$	
	base	w/o g	w/ SVP (C)	w/ SVP (CVQ)	w/ SVP (C)	w/ SVP (CVQ)
<i>RefCOCO</i>						
bbox-test	9.53	3.57	18.99	26.96	20.74	25.52
bbox-testA	5.91	1.59	11.14	14.37	12.33	14.00
bbox-testB	12.35	6.27	25.13	36.65	27.64	34.71
bbox-val	9.93	3.95	18.84	27.01	21.07	25.76
seg-test	9.46	3.70	18.27	25.02	19.68	23.89
seg-testA	5.32	1.37	9.48	12.67	10.95	11.70
seg-testB	12.92	6.44	25.49	35.08	26.61	33.28
seg-val	9.44	4.02	18.35	25.15	19.60	23.95
<i>RefCOCO+</i>						
bbox-testA	6.68	2.16	12.25	16.93	14.05	16.44
bbox-testB	10.98	6.21	23.31	33.02	25.46	30.98
bbox-val	9.57	3.68	18.00	26.67	20.70	25.35
seg-testA	5.98	1.86	10.74	13.97	12.30	13.56
seg-testB	11.75	6.45	23.67	31.25	24.59	29.70
seg-val	9.19	3.90	17.15	24.31	19.13	23.81
<i>RefCOCog</i>						
bbox-test	20.27	13.68	47.74	59.74	50.89	56.79
bbox-val	19.70	12.16	47.69	59.65	50.73	56.81
seg-test	18.76	12.90	45.23	54.39	47.51	51.18
seg-val	18.77	12.55	45.45	54.01	46.93	50.77

Table 12. Evaluation of referring expression generation on various RefCOCO, RefCOCO+, and RefCOCog datasets using LLaVA-1.6-7b. The experiment compares the performance of different models, including a base model, a model without visual grounding (w/o g), a model with Visual Projections (w/ SVP (C)), and a model with SVP and Visual Query (w/ SVP (CVQ)). The performance is measured using the CIDEr score on bounding box (bbox) and segmentation (seg) referring task on the test and validation sets for each dataset. The results show that SVP models significantly outperform the base and w/o g models, indicating the importance of visual grounding for referring tasks. Notice that the adapted models do not have access to the bounding boxes during fine-tuning.

#### D.4. Iteration Ablation

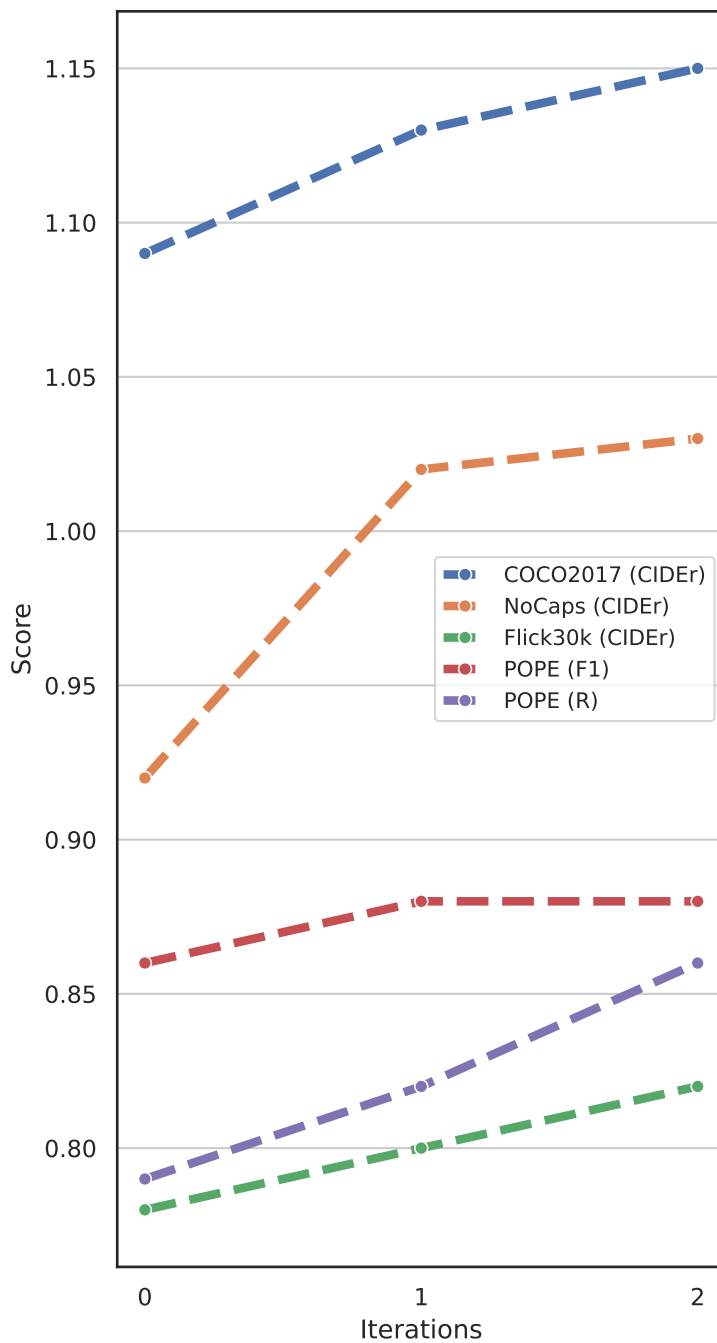


Figure 15. *SVP* effectively boosts captioning performance and reduces hallucinations on benchmark tasks using LLaVA-1.6-7b as base model. The second iteration of *SVP* adaptation leads to significant improvements compared to the initial round, underscoring the value of this technique for enhancing visual-language model capabilities. However, the gains tend to plateau after the second iteration, suggesting diminishing returns from further fine-tuning.

### D.5. Model Size Ablation

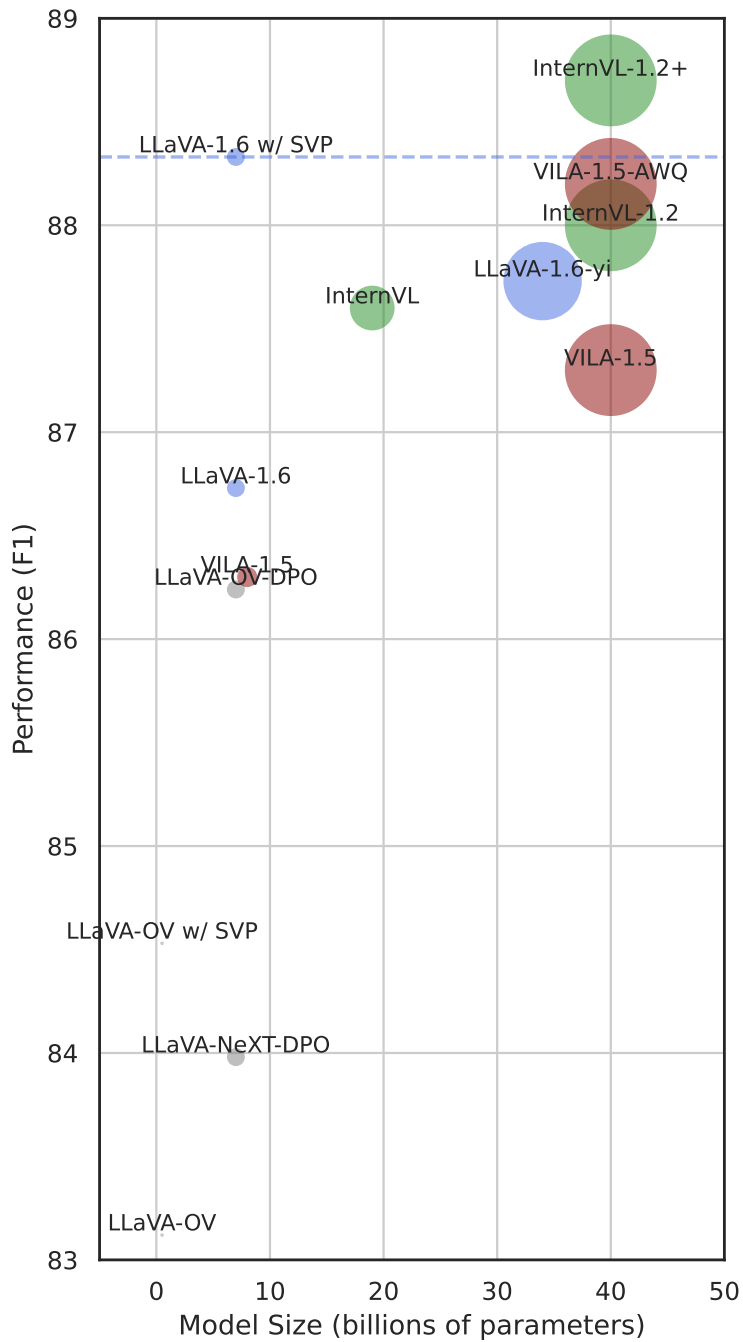
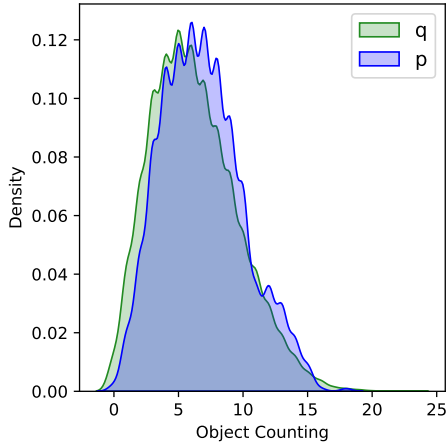
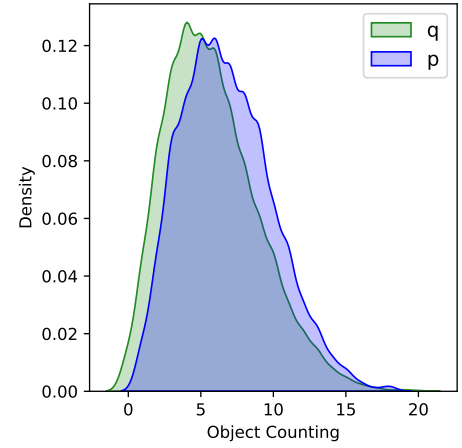


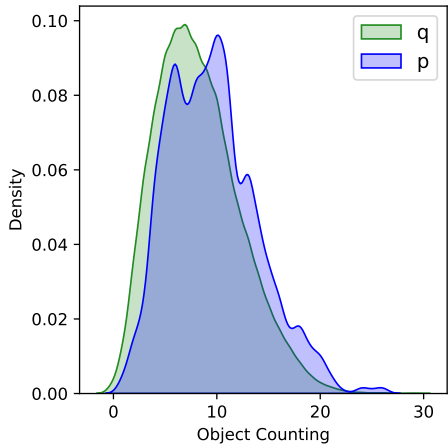
Figure 16. Model size comparison using the F1 metric on the POPE dataset. SVP improves the base model and achieves better or comparable performance with models five times larger.



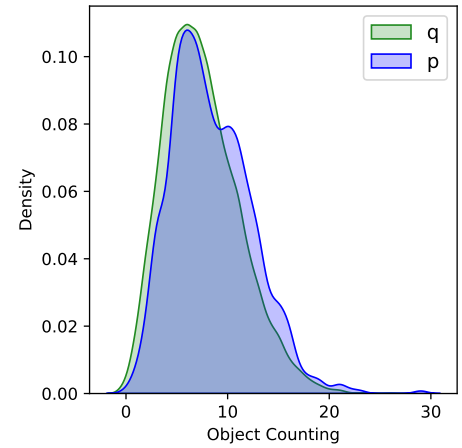
(a) LLaVA-1.5-7b.



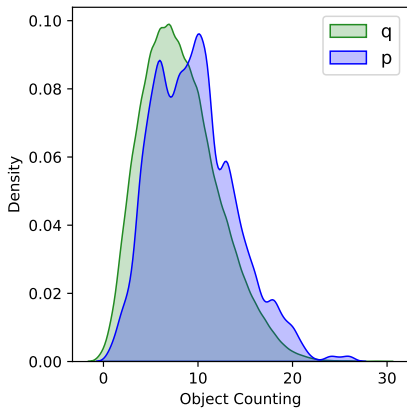
(b) LLaVA-1.5-13b.



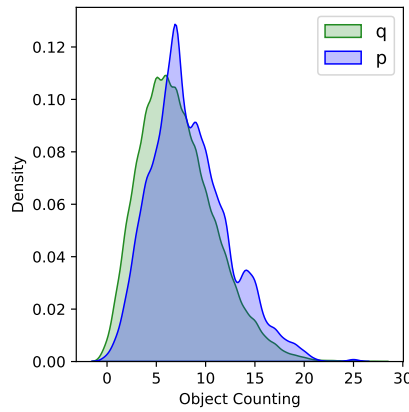
(a) LLaVA-1.6-7b.



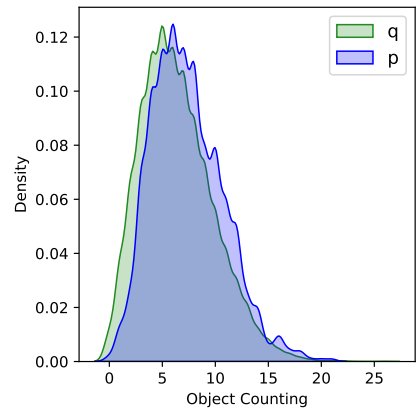
(b) LLaVA-1.6-13b.



(a) LLaVA-1.6-7b iteration 1.



(b) LLaVA-1.6-7b iteration 2.



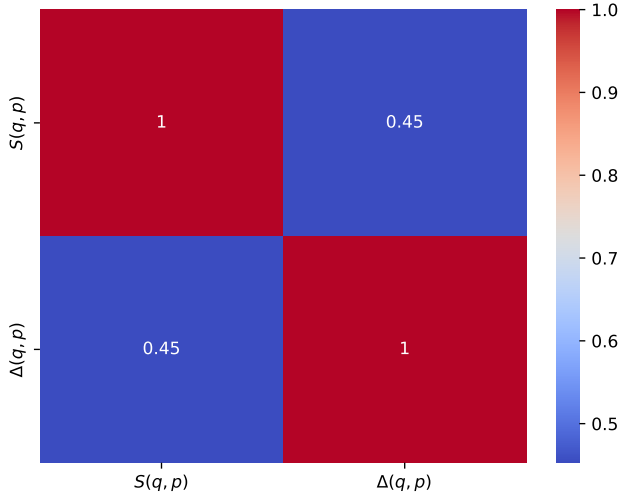
(c) LLaVA-1.6-7b iteration 3.

Figure 19. Distribution of groundable objects in generated caption sampling the base model  $p_{\theta}(\mathbf{z}|\mathbf{c})$  and the grounded model  $q(\mathbf{z}|\mathbf{c}, \mathbf{g})$ . Models adapted with SVP generate less groundable objects and have better object recall.

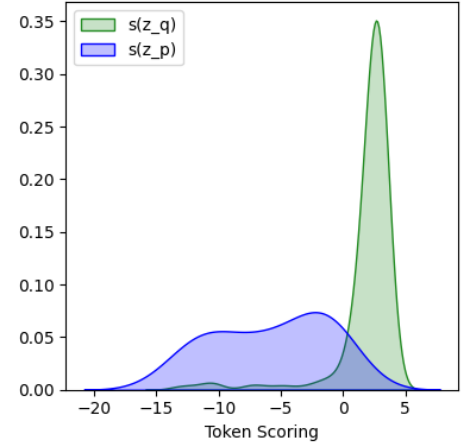
## D.6. Object Grounding Ablation



## D.7. Score Ablation



(a) **Top1 Ranking Correlation** for entropy-based  $\Delta(q, p)$  and kl-based  $S(q, p)$  score using LLaVA-1.6-7b as base model.



(b) **Empirical Distribution** of sequence scores. Log-space representation of  $S(q, p_\theta)$  for sequence scoring. We see the scoring mechanism’s effectiveness to differentiate between posterior samples  $\mathbf{z}_q$  (with grounding) and prior samples  $\mathbf{z}_p$  (without grounding).

Model	Scoring	Adaptation	ScienceQA	VQA	GQA	NoCaps	Captioning	Flickr30k	Referring	Multitasking		Hallucinations	
			test	VQAv2 val_lite	lite	val_lite	COCO2017 val_lite	test_lite	RefCOCO-bbox val_lite	MMBench en_dev_lite	MMMU val	POPE (F1) all	POPE (R) all
LLaVA-1.6-7b	-	-	78.54	<b>76.68</b>	<b>75.80</b>	92.60	109.68	78.74	6.70	<b>80.30</b>	34.11	86.73	79.60
LLaVA-1.6-7b	$\Delta(q, p)$	SVP (C)	77.24	74.98	73.80	100.93	112.95	83.49	18.15	77.27	36.44	<b>88.33</b>	<b>84.20</b>
LLaVA-1.6-7b	$\Delta(q, p)$	SVP (CVQ)	<b>78.40</b>	75.18	<b>75.10</b>	<b>103.95</b>	<b>115.02</b>	<b>85.31</b>	<b>24.74</b>	78.03	<b>37.44</b>	<b>88.25</b>	<b>84.41</b>
LLaVA-1.6-7b	$S(q, p)$	SVP (C)	77.08	75.28	73.28	103.13	113.46	82.57	19.11	76.51	36.44	88.14	83.30
LLaVA-1.6-7b	$S(q, p)$	SVP (CVQ)	78.07	76.04	74.00	102.46	113.73	84.46	21.95	80.30	37.33	88.55	84.46
LLaVA-1.6-13b	-	-	70.30	<b>77.26</b>	<b>74.60</b>	83.89	104.21	69.86	<b>29.71</b>	<b>83.33</b>	35.22	86.24	78.13
LLaVA-1.6-13b	$\Delta(q, p)$	SVP (C)	<b>74.34</b>	76.60	<b>74.40</b>	87.09	111.09	71.43	28.93	81.06	<b>36.33</b>	<b>87.44</b>	81.20
LLaVA-1.6-13b	$\Delta(q, p)$	SVP (CVQ)	68.49	76.26	73.20	<b>100.26</b>	<b>122.03</b>	<b>85.32</b>	27.20	78.03	35.66	<b>87.68</b>	<b>82.53</b>
LLaVA-1.6-13b	$S(q, p)$	SVP (C)	74.44	75.92	73.42	88.46	109.27	70.61	27.73	81.81	35.88	87.06	80.66
LLaVA-1.6-13b	$S(q, p)$	SVP (CVQ)	53.76	75.62	73.80	100.65	118.45	83.63	26.78	77.27	35.22	86.36	81.86

Table 13. Performance using different scoring mechanisms on Vision-Language Benchmarks.  $\Delta(q, p)$  represents a scoring mechanism based on the differential between entropy.  $S(q, p)$  represents a scoring mechanism based on the log ratio output distribution for a VLM w/ and w/o grounding. The table compares the results of different LLaVA model configurations, with varying model sizes (7B and 13B), visual and text encoders (CLIP and Mistral/Vicuna), and adaptation techniques (SVP and SVP with VQ). The results are shown across multiple datasets for each task. We consider scienceQA, VQAv2 and GQA for vision-question answers. NoCaps, COCO2017, Flickr30k for captioning, and RefCOCO for referring. MMBench, and MMMU for multitasking, and POPE for measuring hallucinations. We use CIDEr scores for captioning and referring, accuracy for VQA and multitasking, and F1 and Recall for hallucination tasks. Higher is better for all the metrics. we average over three runs. In each run, we sample a random subset of  $C = 1000$  natural images from the COCO2014 training set [59].

## D.8. DPO Ablation

Model	Samples	SciQA	VQAv2	GQA	NoCaps	COCO2017	Flickr30k	RefCOCO	MMBench	MMMU	POPE
LLaVA-7b-OV w/ DPO	$\geq 9.4k$	79.25	79.68	72.80	112.51	135.32	85.27	13.60	85.60	48.66	86.21
LLaVA-7b-OV w/ SVP	$\approx 2k$	83.89	78.82	73.40	120.23	137.07	83.37	15.75	86.36	49.33	85.78

Table 14. Comparison between SVP and DPO [78] for LLaVA-7b-OV on the lite benchmark. DPO is an effective method to improve alignment with human-preference and reduce hallucination. But it can reduce performance for captioning, multitasking, referring, and visual question answering.

## E. Connection with Latent Variable Models

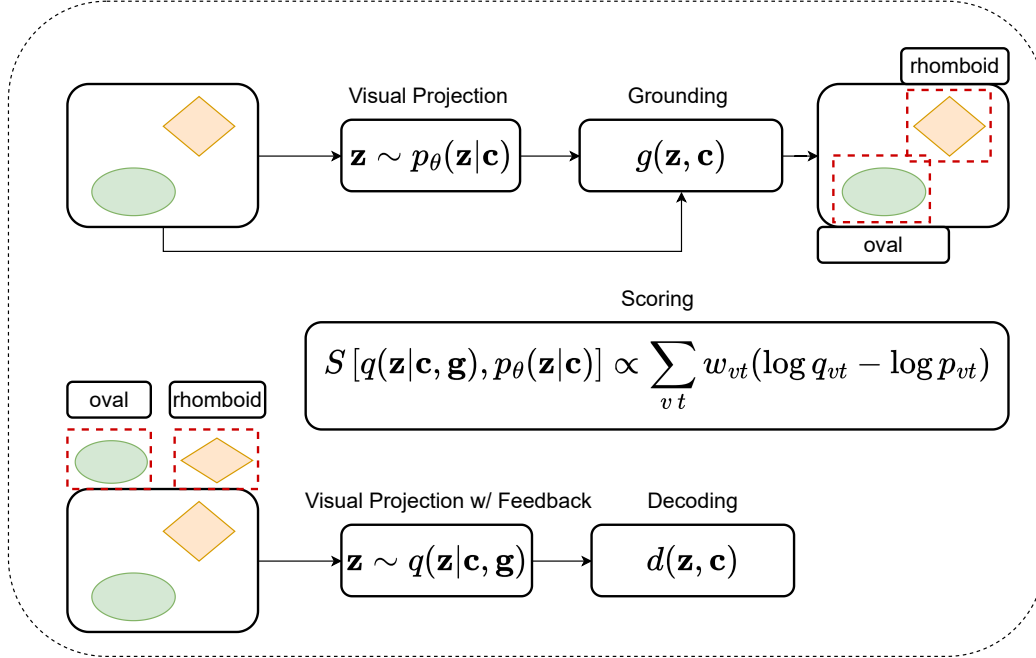


Figure 21. **SVP with grounded sampling and scoring.** The Inner-loop is repeated  $K$  times and consists of the following steps: (i) Sampling: We generate samples both with and without grounding. (ii) Scoring and Re-ranking: The generated samples are evaluated and reordered based on their scores. (iii) Filtering: We select the top  $k$  samples from the re-ranked set. The loop incorporates data generation, uses grounding as feedback, and filters for divergence. Importantly, we take a novel approach to grounding: instead of visual representation, we convert the grounding information into text and append it to the prompt as additional context. This method projects grounding directly into the text space, thereby simplifying the alignment between modalities.

A  $VLM_{\theta}$  can be represented as a conditional distribution:

$$p_{\theta}(\mathbf{x}|\mathbf{c}) = \int p_{\theta}(\mathbf{x}|\mathbf{z}, \mathbf{c}) p_{\theta}(\mathbf{z}|\mathbf{c}) d\mathbf{z} = \mathbb{E}_{p_{\theta}(\mathbf{z}|\mathbf{c})} [p_{\theta}(\mathbf{x}|\mathbf{z}, \mathbf{c})]. \quad (5)$$

The input conditioning information is represented by  $\mathbf{c} = (\mathbf{c}_v, \mathbf{c}_t)$ , while  $\mathbf{x}$  denotes the model output, which could be an answer to a question or a caption. In scenarios where our output is a classification or regression target, we can approximate the decoding distribution  $p_{\theta}(\mathbf{x}|\mathbf{z}, \mathbf{c})$  using a deterministic function:  $p_{\theta}(\mathbf{x}|\mathbf{z}, \mathbf{c}) = \delta(\mathbf{x} - d_{\theta}(\mathbf{z}, \mathbf{c}))$ . In this context,  $\mathbf{z}$  represents a latent (or visible) variable that encapsulates a detailed and comprehensive description of the visual information. It serves as a visual projection that fully describes the objects and relationships present in the visual input through output text. Given that VLMs are typically constructed using discrete tokens, we can assume the latent information follows a categorical or multinomial distribution. This allows us to rewrite our formulation as follows:

$$p_{\theta}(\mathbf{x}|\mathbf{c}) = \sum_{\mathbf{z}} p_{\theta}(\mathbf{x}|\mathbf{z}, \mathbf{c}) p_{\theta}(\mathbf{z}|\mathbf{c}). \quad (6)$$

Our primary objective is to develop a better prior  $p_{\theta}(\mathbf{z}|\mathbf{c})$  that more effectively captures visual information. This approach aims to eliminate the need for collecting an expensive and error-prone dataset of grounded and optimized captions. By doing so, we can enhance the model’s ability to understand and represent visual content without relying on manual annotation processes.

**MAP Estimation** A simple approach is to leverage additional conditional information leveraging grounding. This strategy involves incorporating context to enhance the model’s understanding of visual content. Specifically, we might consider the following forms of conditional information:

$$p_\theta(\mathbf{x}|\mathbf{c}, \mathbf{g}) = \int p_\theta(\mathbf{x}|\mathbf{z}, \mathbf{c})p_\psi(\mathbf{z}|\mathbf{c}, \mathbf{g}) d\mathbf{z} \quad (7)$$

where  $\mathbf{g} = g(\mathbf{c}_v, \mathbf{z}_\theta)$ , which represents the output of a grounding model  $g$ . This model serves to provide crucial feedback, taking as input the visual information  $\mathbf{c}_v$  and samples from the prior model  $\mathbf{z}_\theta$ . We can then approximate this model using a Maximum a Posteriori (MAP [10]) estimator. This leads us to a formulation that can be expressed as:

$$\int p_\theta(\mathbf{x}|\mathbf{z}, \mathbf{c})p_\psi(\mathbf{z}|\mathbf{c}, g(\mathbf{c}_v, \mathbf{z}_\theta))d\mathbf{z} \approx p_\theta(\mathbf{x}|\mathbf{z}_\psi(\mathbf{c}, g(\mathbf{c}_v, \mathbf{z}_\theta)), \mathbf{c}). \quad (8)$$

This approach, inspired by meta-learning [31], is in principle feasible. Following our notation in Fig. 2,  $\psi$  and  $\mathbf{z}_\psi(\mathbf{c}, g(\mathbf{c}_v, \mathbf{z}_\theta))$  represent the inner-loop, while  $\theta$  and  $p_\theta(\mathbf{x}|\mathbf{z}_\psi(\mathbf{c}, g(\mathbf{c}_v, \mathbf{z}_\theta)), \mathbf{c})$  correspond to the outer-loop. However, this straightforward approach has a significant drawback - it necessitates reliance on the grounding model at inference time. Ideally, grounding should only be utilized in the inner-loop to generate improved prior samples  $\mathbf{z}$ . The VLM should indirectly acquire such information through the outer-loop, subsequently generalizing to a wide range of tasks without explicitly requiring grounding information after adaptation.

**Rethinking Posterior Inference** We can follow an alternative approach to enhance the model’s output through grounding. We can define a posterior distribution  $q(\mathbf{z}|\mathbf{c}, \mathbf{g})$ , where  $\mathbf{g}$  represents external feedback. This feedback could be provided by a pre-trained, computationally efficient grounding model denoted as  $g(\mathbf{c}_v, \mathbf{z})$ . By incorporating posterior inference, we can formulate a variational lower bound [43, 49] as follows:

$$\mathbb{E}_{q(\mathbf{z}|\mathbf{c}, \mathbf{g})} [\log p_\theta(\mathbf{x}, \mathbf{z}|\mathbf{c}) - \log q(\mathbf{z}|\mathbf{c}, \mathbf{g})]. \quad (9)$$

This bound formulation, while challenging to train for a VLM, is easy to evaluate. This intuition suggests the following algorithm: for a given input  $\mathbf{c}$ , we first run the posterior distribution  $q$  with grounding feedback to generate logits for each element  $v$  in the vocabulary  $V$  and each generated token  $t$  in the sequence  $T$ . We then run the base model to perform the same computations, obtaining the prior distribution  $p_\theta$ . This approach allows us to incorporate grounding feedback indirectly into the model, potentially leading to more contextually appropriate and visually grounded outputs. By comparing the posterior distribution (informed by the grounding model) with the prior distribution (the base model), we can create a bridge between the visual input, the language model, and the external grounding information, better aligning visual and language modalities without requiring feedback at inference time.

**Divergence-based Scoring** To estimate the impact of the grounding feedback, we can utilize the log-ratio between the posterior and prior distributions, weighted by the posterior. This approach can be formalized as follows:

$$\mathbb{D}[q, p] \propto \sum_t \sum_v q_{v,t}(\mathbf{z}|\mathbf{c}, \mathbf{g}) [\log q_{v,t}(\mathbf{z}|\mathbf{c}, \mathbf{g}) - \log p_{\theta_{v,t}}(\mathbf{z}|\mathbf{c})]. \quad (10)$$

Using this formulation, we can build the following score:

$$S[q, p] = \sum_t \gamma_t \sum_v w_{v,t} [\log q_{v,t}(\mathbf{z}|\mathbf{c}, \mathbf{g}) - \log p_{\theta_{v,t}}(\mathbf{z}|\mathbf{c})] = \sum_t \gamma_t \sum_v S_{v,t}[q, p], \quad (11)$$

where

$$S_{v,t}[q, p] = w_{v,t} [\log q_{v,t}(\mathbf{z}|\mathbf{c}, \mathbf{g}) - \log p_{\theta_{v,t}}(\mathbf{z}|\mathbf{c})]. \quad (12)$$

We can also define a normalized version:

$$S[q, p, \mathbf{z}_t] = \frac{\sum_t \gamma_t S_{v,t}[q, p]|\mathbf{z}_t}{\sum_t \gamma_t \sum_v S_{v,t}[q, p]} = \frac{\sum_t \gamma_t S_{v,t}[q, p]|\mathbf{z}_t}{S[q, p]}. \quad (13)$$

The impact of grounding feedback can be modulated using a factor  $\gamma_t \in [0, 1]$ , which accounts for both the sequence length and the distance of a text token from the last visual token. In this formulation,  $\mathbf{z}_{\bar{v},t} = \mathbf{z}_t$  represents the visual projection at step  $t$  of the generated sequence for element  $\bar{v}$  in the vocabulary. We collect pairs  $(\mathbf{z}, \mathbf{c})$  where the divergence between the posterior and prior distributions exceeds a certain threshold. These pairs are then used to fine-tune the base model. The underlying

principle is that significant differences between  $q$  and  $p$  are likely caused by the grounding conditioning  $g$ . Small values of  $S[q, p]$  indicate token trajectories that the base model  $p$  already comprehends well, thus providing little additional information. Conversely, large values of  $S[q, p]$  represent trajectories that surprise the base model across the vocabulary. These instances of surprise potentially offer valuable feedback and additional information to enhance the visual projection. This approach allows us to selectively fine-tune our model on the most informative examples, potentially leading to more efficient learning and better integration of visual and textual information. By focusing on areas where the grounding model significantly influences predictions, we can enhance the model’s ability to generate visually coherent and contextually appropriate text.

**Adaptation** Finally, we can adapt the base model  $p_\theta$  on the collected trajectories using:

$$\mathbf{z}_G \sim q(\mathbf{z}|\mathbf{c}, \mathbf{g}) \quad \mathbb{E}_{q(\mathbf{x})q(\mathbf{z}_G)} \log p_\theta(\mathbf{x}, \mathbf{z}_G|\mathbf{c}) \tag{14}$$

In this context,  $\mathbf{x}$ , the output variable, could represent an answer to a question. More broadly, we can consider  $\mathbf{x}$  as a continuation generated from  $\mathbf{z}$ , such as additional reasoning or more detailed information. Given our objective of developing a model capable of generalizing to various tasks, we treat  $\mathbf{x}$  as a generic continuation. This continuation could be deterministic, or in the boundary case where  $\mathbf{x} = I(\mathbf{z})$ , we can directly consider  $\mathbf{z}$  as observable.

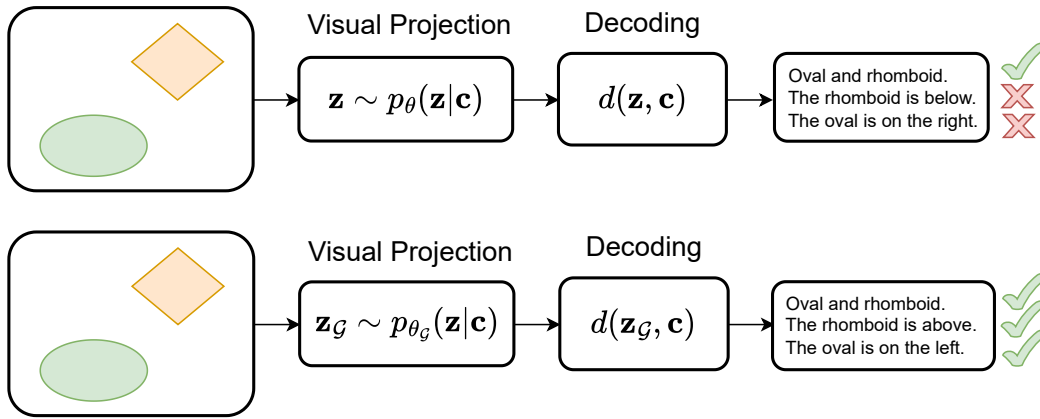


Figure 22. **Inference with Vision-Language Models.** Top) Standard inference. Bottom) Adapted inference with SVP.

**Grounding as Vision-Language Alignment** Visual grounding can be conceptualized as the dual of text-image alignment. When viewed as a mechanism to extract and structure information within a VLM, grounding essentially functions as a form of alignment between visual and textual modalities. This alignment is a critical component in both LLMs and VLMs, with the primary objective being to develop a unified representational space that facilitates effective cross-modal interaction and reasoning. The modality alignment process is often multi-faceted, encompassing pre-training on extensive datasets, fine-tuning for specific tasks, and the application of techniques like preference tuning and contrastive learning. These methods aim to encourage the model to learn meaningful correspondences across modalities. Modality alignment is the key to unlocking the full potential of VLMs in tasks that require integration of visual and textual information. By establishing a robust alignment between these modalities, VLMs can more effectively process, understand, and generate responses that coherently combine visual and linguistic elements, thereby enhancing their performance across a wide range of applications.

## F. Prompting

### System Prompt - Sampling

You are an AI visual-language assistant that can analyze images and helps writing detailed descriptions of images.

```
<instruction>
```

Describe the scene and the objects in the image in details. Describe the object attributes and positions. Output only the descriptions of objects that are in the image. Use separate sentence for each object.

Include details like object counts, position of the objects, relative position between the objects.

Start your description with "In the image, ".

```
</instruction>
```

### System Prompt - Grounded Sampling

You are an AI visual-language assistant that can analyze images and helps writing detailed descriptions of images.

In addition, specific objects and object locations within the image are given, along with detailed coordinates inside `<context></context>`. These coordinates are in the form of bounding boxes, represented as  $(x1, y1, x2, y2)$  with floating numbers ranging from 0 to 1. These values correspond to the top left  $x$ , top left  $y$ , bottom right  $x$ , and bottom right  $y$ .

```
<instruction>
```

Using the provided objects and bounding boxes inside `<context></context>`, describe the image.

Describe the scene and the objects in the image in details. Describe the object attributes and positions. Output only the descriptions of objects that are in the image. Use separate sentence for each object.

Include details like object counts, position of the objects, relative position between the objects.

*Do not mention the bounding box coordinates. Utilize this data to explain the scene using natural language.*

Start your description with "In the image, ".

```
</instruction>
```

### Base Prompt

Please generate a detailed and comprehensive description for the content of this image. Be precise.

### Grounded Prompt

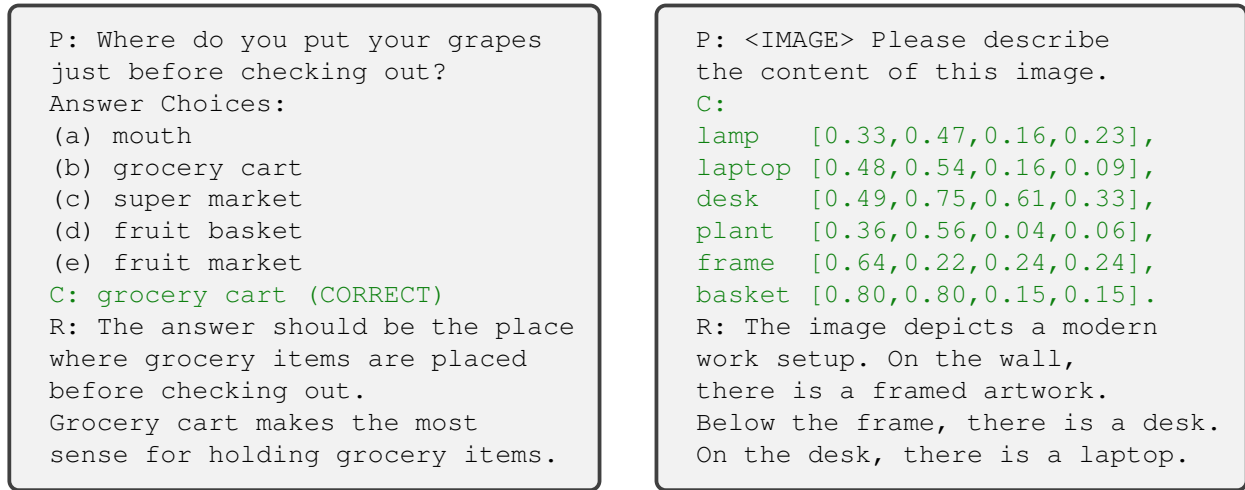
```
<context>
{grounding}
</context>
```

Please generate a detailed and comprehensive description for the content of this image. Be precise.

## G. Connection with iterative Improvement in LLMs

### G.1. Self-Taught Reasoner

Our method is inspired by recent advances in self-improvement in language modelling [24, 32, 117], where the focus has been in improving chain-of-thought reasoning leveraging feedback. The Self-Taught Reasoner (STaR [117]) uses ground truth labels and rationalization as feedback [117] and fine-tunes the model on reasoning steps that generate the correct answer [36]. In Fig. 23 we provide a comparison between SVP and rationalization in STaR, where the model tries to find the correct reasoning path given external feedback in the form of a ground truth response.



(a) Rationalization in STaR. We sample from  $q(\mathbf{z}|\mathbf{c}, \mathbf{y})$ , where  $\mathbf{y}$  is the ground truth label provided as context  $C$ . The response  $\mathbf{z}$  is then leveraged to build  $p(\mathbf{y}|\mathbf{c}, \mathbf{z})$  or a deterministic decoding  $d(\mathbf{c}, \mathbf{z})$ .

(b) Grounded sampling in SVP. We sample from  $q(\mathbf{z}|\mathbf{c}, \mathbf{g})$ , where  $\mathbf{g}$  is the grounding information provided as context  $C$ . The response  $\mathbf{z}$  is then leveraged to build  $p(\mathbf{x}|\mathbf{c}, \mathbf{z})$  or a deterministic decoding  $d(\mathbf{c}, \mathbf{z})$ .

Figure 23. Comparison between rationalization in STaR [117] and posterior sampling in SVP.

### G.2. Connections with RLHF and DPO

In this subsection we briefly show how recent methods for aligning and improving language models [78, 128] can be re-written using our notation.

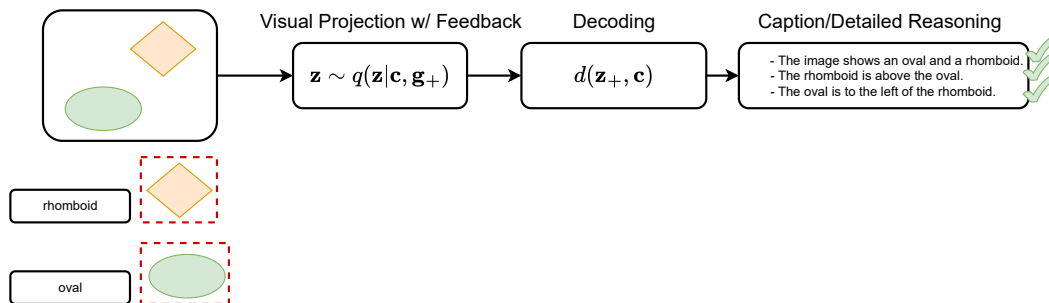


Figure 24. Grounded Visual Projection. These samples can be used as positive.

**Reinforcement Learning with Preference Feedback** Reinforcement Learning from Human Feedback (RLHF [20, 128]) is an algorithm that combines Reinforcement Learning (RL) with human preferences. Often implemented using Proximal Policy Optimization (PPO [86]), RLHF aims to align AI models with human values. At its core, RLHF involves two key components: (i) a reward model  $s_\phi$ , which encodes a set of predefined preferences, typically derived from human labelling [13, 20]. (ii) A

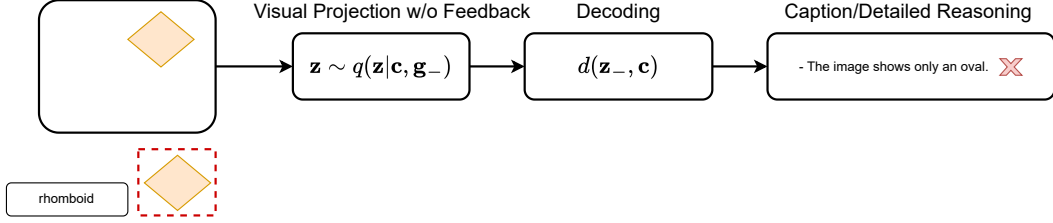


Figure 25. "Ungrounded" Visual Projection. These samples can be used as negative.

policy model  $q_\phi$ , which is iteratively improved based on the feedback from the reward model, enhancing the capabilities of the initial base model  $p_\theta$ .

$$\mathcal{F}_{\text{RL}} = \mathbb{E}_{q_\phi(\mathbf{z}|\mathbf{c}, \mathbf{g})} \left[ s_{\bar{\psi}}(\mathbf{z}_\phi, \mathbf{c}, \mathbf{g}) - \gamma \log \frac{q_\phi(\mathbf{z}|\mathbf{c}, \mathbf{g})}{p_\theta(\mathbf{z}|\mathbf{c})} \right] \quad (15)$$

While traditional RL algorithms like REINFORCE [106] can be unstable, PPO addresses this issue by introducing a proximity constraint. This constraint penalizes significant deviations of the improved model  $q_\phi$  from the base model  $p_\theta$ , measured using a  $\mathbb{KL}$  divergence. The RLHF process involves several steps: (i) Generating samples  $\mathbf{z}$  from the current policy model  $q_\phi$ . (ii) Evaluating these samples using the reward model  $s_{\bar{\psi}}$ . (iii) Updating the policy model, maximizing the reward while considering the regularization term involving  $p_\theta$ . This iterative process, while effective, is computationally intensive, requiring substantial memory and sampling resources. Despite these challenges, RLHF has proven to be a powerful method for aligning AI systems with human preferences, leading to significant improvements in chat applications of language models.

**Direct Preference Optimization** Direct Preference Optimization (DPO [78]) offers a novel approach to language model fine-tuning that eschews sampling techniques, presenting several advantages over RLHF methods. DPO simplifies the process by (i) eliminating the need for an explicit reward or scoring model, instead (ii) relying on a set of labelled positive and negative examples, and (iii) achieving greater stability and efficiency in the fine-tuning process. DPO utilizes the log-ratio between the policy model  $q_\phi$  and the base model  $p_\theta$  to define an implicit reward  $s_\psi$ , constructed using positive and negative samples.

$$\mathcal{F}_{\text{DPO}} = \mathbb{E}_{q_\phi(\mathbf{z}|\mathbf{c}, \mathbf{g})} \log \sigma \left[ \gamma \left( \log \frac{q_\phi(\mathbf{z}|\mathbf{c}, \mathbf{g}^+)}{p_\theta(\mathbf{z}|\mathbf{c})} - \log \frac{q_\phi(\mathbf{z}|\mathbf{c}, \mathbf{g}^-)}{p_\theta(\mathbf{z}|\mathbf{c})} \right) \right] \quad (16)$$

This implicit reward serves as feedback to enhance the model  $q_\phi$ , effectively improving upon the base model  $p_\theta$ . Unlike RLHF, which requires online sampling from the model, DPO allows for the use of standard cross-entropy loss for classification to optimize the parameters  $\phi$ . By leveraging paired samples and avoiding expensive sampling strategies, DPO offers a simpler and potentially more robust method for aligning language models with human preferences. See [41] for an extensive comparison between DPO and RLHF.

## H. Visualizations

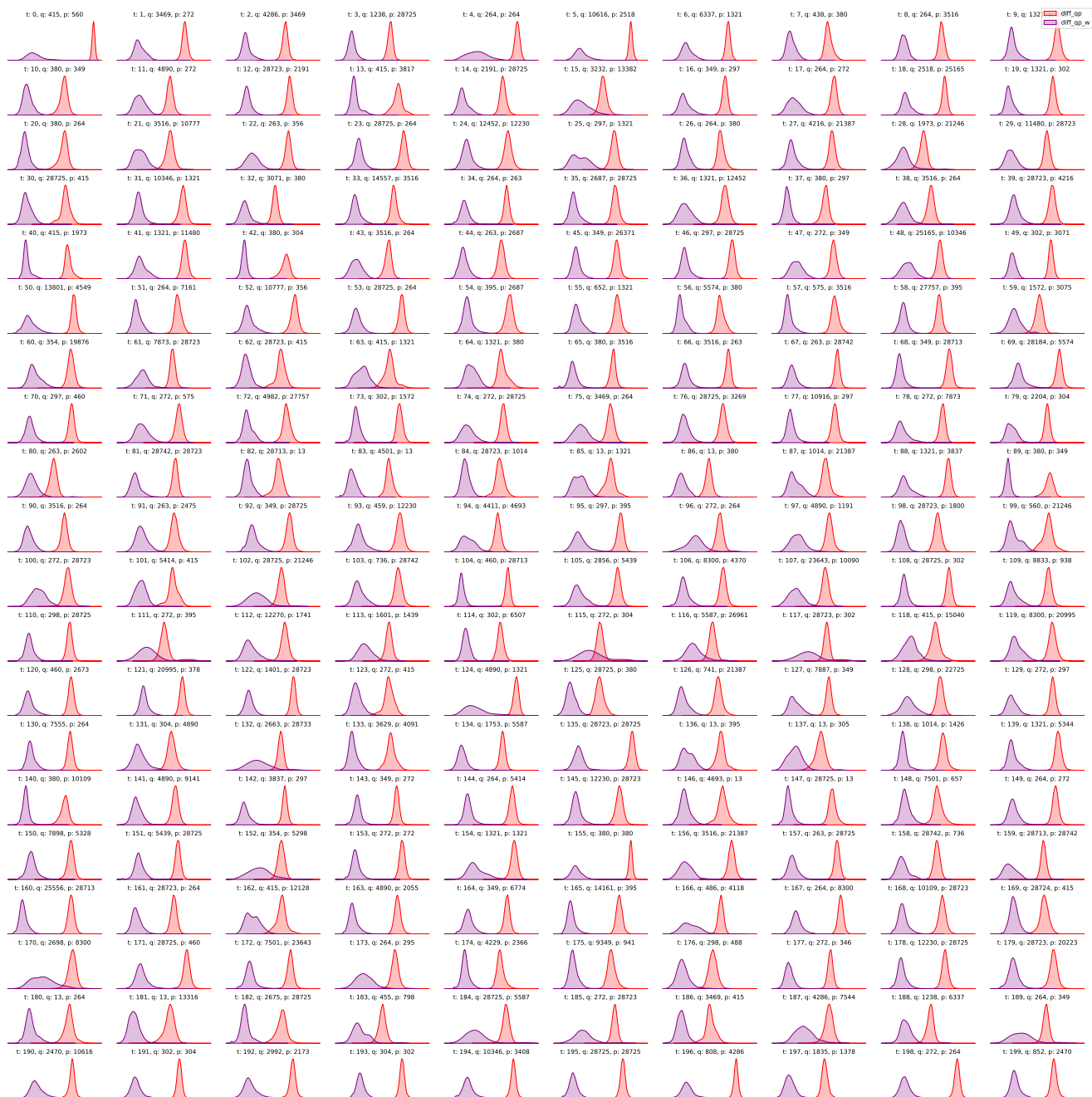


Figure 26. Conditional log-difference w/ and w/o weighting for  $q$  and  $p$  over the vocabulary  $V$  for  $T$  tokens in a generated sequence.



**Instruction:** Describe the content of this image as detailed as possible.



**VLM response w/o SVP:**

In the image, there are **four pizzas** in an oven. The oven is filled with racks, each holding a pizza. The pizzas are of different types, with various toppings visible. The oven is illuminated, casting a warm glow on the pizzas. The pizzas are arranged in two rows, with **two pizzas in each row**. The pizzas are cooking, as indicated by their position in the oven. The oven is a standard kitchen appliance, with a door that is open to reveal the pizzas inside. The pizzas are the main focus of the image, with their colors and textures contrasting against the dark interior of the oven. The image captures a moment of culinary preparation, with the pizzas in various stages of cooking.

**VLM response w/ SVP:**

In the image, there is a well-lit oven with a black interior. Inside the oven, there are **three pizzas** on the top rack and **two pizzas** on the bottom rack. On the top rack, the first pizza is on the left side of the oven. It has a golden brown crust and is topped with green peppers and mushrooms. The second pizza is on the right side of the oven. It also has a golden brown crust and is topped with green peppers and black olives. On the bottom rack, the first pizza is on the left side of the oven. It has a golden brown crust and is topped with mushrooms. The second pizza is on the right side of the oven. The light inside the oven illuminates the pizzas, highlighting their toppings and crusts. The pizzas appear to be freshly baked, as their crusts are golden brown and their toppings are evenly distributed. The overall scene suggests a home or restaurant kitchen where pizzas are being prepared.

**Instruction:** Describe the content of this image as detailed as possible.



**VLM response w/o SVP:**

In the image, there is a large clock mounted on a building. The clock face is white with black numbers and hands. The building itself is adorned with intricate carvings and statues. There are three statues visible in the image. One statue is of a woman holding a shield, another is of a man holding a spear, and the third is of a man holding a scroll. The carvings and statues are detailed and appear to be made of stone. The building has a gray roof, and the clock is positioned in the center of the image. The statues are positioned on either side of the clock, with the woman on the left, the man with the spear in the middle, and the man with the scroll on the right. The overall scene is a blend of architectural and artistic elements.

**VLM response w/ SVP:**

In the image, there is a grand clock tower that is ornate and intricate. The tower is made of stone and is topped with a statue of a woman holding a sword. This statue is located at the top of the tower, near the center. The tower also features a large clock face on the front, which is situated below the statue. The clock face is white with black numbers and hands. Below the clock face, there are two smaller statues of people. These statues are positioned on either side of the clock face, with the one on the left being slightly larger than the one on the right. The tower is set against a gray brick background, which contrasts with the white stone of the tower. The overall scene suggests a sense of grandeur and history.

## I. Qualitative Examples

Here we provide additional visualizations and examples to illustrate our method. The images used for captioning and visual queries were selected from the COCO2014 training set [59], while referring examples were sourced from the RefCOCO dataset [46], specifically the val\_lite set [123]. The examples are presented with minimal post-processing, limited to the removal of special characters and correction of obvious grammatical errors. Both models were prompted using the protocols outlined in Appendix F. All hyper-parameters remained consistent across both models. The examples compare output of LLaVA-1.6 models sampling from the base model (w/o SVP) and sampling from the adapted model (w/ SVP). These comparisons provide qualitative insights into the performance differences between the base and adapted models.

### I.1. Captioning Tasks

**Instruction:** Describe the content of this image as detailed as possible.



**VLM response w/o svp:**

In the image, there are three objects: a pink frisbee, a pair of red sneakers, and a beer bottle. The pink frisbee is located in the foreground, with its star-shaped design prominently displayed. The red sneakers are positioned in the background, with one shoe slightly in front of the other. The beer bottle is also in the background, standing upright and slightly to the right of the sneakers. The objects are arranged in a way that suggests a casual, outdoor setting, possibly a park or a beach. The frisbee and sneakers are the main focus of the image, while the beer bottle adds a touch of leisure to the scene.

**VLM response w/ svp:**

In the image, there is a casual outdoor setting with a pair of red and white Adidas shoes. The shoes are placed on a grassy area, with one shoe closer to the camera and the other slightly behind it. The Adidas logo is prominently displayed on both pairs of shoes. A pink frisbee with a blue star design is also present in the scene. It is positioned in the foreground, with the shoes in the background. The frisbee appears to be resting on the grass, and its bright color stands out against the natural backdrop. The overall scene suggests a leisurely outdoor activity, possibly a game of frisbee, with the Adidas shoes indicating a sporty or active lifestyle. The grassy area and the casual arrangement of the shoes and frisbee give the image a relaxed and informal vibe.

**Instruction:** Describe the content of this image as detailed as possible.



James Panaligan  
ジェームス・パナリガン

**VLM response w/o svp:**

In the image, there is a large yellow bus parked on the side of a street. The bus is positioned on the right side of the image and is the most prominent object in the scene. It is a double-decker bus, which is characterized by its two levels of seating. The bus is parked next to a sidewalk, which is visible on the right side of the image. There are several people in the image, some of whom are standing near the bus. One person is standing on the sidewalk, while others are standing on the street. There is also a car parked on the left side of the image, which is partially visible. The bus is parked in front of a building, which is located on the left side of the image. The building is partially visible, with only the top part of it visible in the image. The bus is also parked near a tree, which is located on the left side of the image. The tree is partially visible, with only the top part of it visible in the image. The overall scene suggests a typical day in a city, with people going about their daily routines and public transportation being a common sight.

**VLM response w/ svp:**

In the image, a large yellow bus dominates the scene, traveling down a city street. The bus is vibrant and appears to be in motion, heading towards the right side of the frame. Its size and bright color make it the main focus of the image. In the background, another bus can be seen, albeit much smaller and less prominent. It's positioned on the left side of the image, providing a sense of depth and perspective to the scene. On the right side of the image, there's a large advertisement. It's not clear what the advertisement is for, but its size and placement suggest it's a significant feature of the urban landscape. The setting appears to be a typical city street. Trees can be seen in the background, adding a touch of nature to the urban environment. There are also several people scattered throughout the image, going about their day, which contributes to the everyday, relaxed atmosphere of the scene. The overall composition of the image suggests a bustling city life, with public transportation playing a significant role. The buses, people, and advertisement all come together to paint a picture of a vibrant, active cityscape.

**Instruction:** Describe the content of this image as detailed as possible.



**VLM response w/o SVP:**

In the image, there are three horses standing in a dirt enclosure. The horse on the left is brown with a white blaze on its face. It is standing with its head turned to the side, **looking towards the camera**. The horse in the middle is white with a brown spot on its head. It is standing with its **head turned to the side**, looking towards the camera. The horse on the right is brown with a white blaze on its face. It is standing with its head turned to the side, **looking towards the camera**. The enclosure is made of metal fencing and there is a mountain visible in the background.

**VLM response w/ SVP:**

In the image, there are three horses standing in a dirt enclosure. The horse on the left is brown with a white stripe running down its nose. Its head is slightly turned to the left. The horse in the middle is white and stands with its head facing forward. The horse on the right is black and its head is turned to the right. The three horses are standing next to each other, separated by a metal fence. In the background, there is a clear blue sky and a mountain range. The overall scene is a serene outdoor setting.

**Instruction:** Describe the content of this image as detailed as possible.



**VLM response w/o SVP:**

In the image, there is a young boy standing on the shore of a body of water. The boy is wearing a striped shirt and has blonde hair. He is looking out towards the water, which is calm and reflects the light. In the distance, there is a boat on the water, and the horizon is visible. The boy is standing in **front of a tree with green leaves**, which is located on the shore. The overall scene suggests a peaceful day by the water.

**VLM response w/ SVP:**

In the image, a young boy is standing by a body of water. He is wearing a black striped shirt. His back is turned to the camera, and he is looking out at the water. The boy appears to be standing on a grassy area near the water's edge. The water in the image is calm and appears to be a lake or a large river. It is a clear day, and the sky is visible in the background. There are no other people or objects in the image. The boy is the only person present. The relative position of the boy to the water is such that he is **standing on the right side of the image**. He is standing closer to the foreground than the water, which is further back in the image. The boy is also standing to the **right of the water**.

**Instruction:** Describe the content of this image as detailed as possible.



**VLM response w/o svp:**

In the image, there is a bathroom setting. The main object is a white toilet, which is positioned in the lower right corner of the image. The toilet is situated on a beige tiled floor. Above the toilet, there is a metal rack mounted on the wall. The rack holds a single magazine, which is titled "Architectural Digest". The magazine is displayed prominently on the rack, indicating that it is the main focus of the rack's purpose. The overall scene suggests a well-organized and aesthetically pleasing bathroom space, with the magazine rack providing a functional and decorative element. The white toilet contrasts with the beige tiles, creating a clean and modern look. The magazine on the rack adds a touch of sophistication and suggests an interest in architecture or design.

**VLM response w/ svp:**

In the image, there is a bathroom setting with a white toilet located towards the right side of the frame. Above the toilet, there is a magazine rack mounted on the wall. The rack holds two magazines, one titled "ARCHITECTURAL DIGEST" and the other "EXOTIC HOMES". The "ARCHITECTURAL DIGEST" magazine is positioned slightly higher than the "EXOTIC HOMES" magazine, and both are centrally located within the rack. The "EXOTIC HOMES" magazine is situated directly below the "ARCHITECTURAL DIGEST" magazine. The bathroom walls are beige, and the overall scene suggests a quiet and relaxed atmosphere.

**Instruction:** Describe the content of this image as detailed as possible.



**VLM response w/o svp:**

In the image, there are three giraffes standing in a field. The giraffe on the left is bending its neck down towards the ground, possibly to reach for food or water. The giraffe in the middle is standing upright, with its neck extended upwards. The giraffe on the right is also standing upright, but its neck is bent down towards the ground. All three giraffes are facing the same direction, suggesting they might be looking at something in the distance. The field they are standing in appears to be dry and dusty, with no visible vegetation. There are no other objects or animals in the image.

**VLM response w/ svp:**

In the image, there are three giraffes standing in a field. The giraffes are tall and majestic, with their long necks reaching upwards. The giraffe on the left is slightly bending its neck, possibly to reach for something. The giraffe in the middle is standing upright, and the giraffe on the right is also bending its neck. In the center of the image, there is a tall pole. The pole has a feeder attached to it, which is likely providing food for the giraffes. The pole is surrounded by the field, which appears to be dry and brown. The giraffes are spread out across the image, with the giraffe on the left being closer to the pole than the other two. The giraffe on the right is the furthest away from the pole. The giraffes are the main focus of the image, with their long necks and distinctive patterns standing out against the backdrop of the field.

**Instruction:** Provide a short description for this region.



**VLM response w/o svp:**

The image shows a man sitting in the foreground, looking to the side with a serious expression. Behind him, there is another man standing on a boat, gesturing with his hands. The boat has a lifebuoy with the word "UNDER" on it, and the man standing is wearing a white cap and sunglasses. The background features a clear blue sky and calm water, with a few boats visible in the distance. The overall setting suggests a leisurely day out on the water.

**VLM response w/ svp:**

A man wearing a white hat and sunglasses.

**Instruction:** Provide a short description for this region.



**VLM response w/o svp:**

The image shows a bag of donuts with the brand name "NATAS" printed on it. The donuts are visible through the clear plastic packaging, and there are three donuts in total. The donuts appear to be of a similar type, possibly a ring donut, and they are placed on a white surface. The background is blurred, but there is a hint of a beige or light brown object to the right of the bag. The text on the bag is in Japanese, and the donuts have a hole in the center, which is typical for ring donuts.

**VLM response w/ svp:**

A donut in a bag.

## I.2. Referring Tasks

**Instruction:** Provide a short description for this region.



**VLM response w/o svp:**

The image shows a person holding a mug with a flamingo design. The mug features two flamingos, one pink and one white, surrounded by green foliage and blue flowers. The design is colorful and playful, with the flamingos depicted in a stylized manner. The mug has a white handle and is placed in front of a computer keyboard, suggesting that the person might be using the computer while enjoying their drink. The background is blurred, but it appears to be an indoor setting with a desk or table.

**VLM response w/ svp:**

A white coffee mug with a flamingo design.

**Instruction:** Provide a short description for this region.



**VLM response w/o svp:**

The image is a black and white photograph capturing a moment on a tennis court. In the foreground, there are two men standing on the court. The man on the left is holding a tennis racket and appears to be speaking into a microphone, suggesting he might be a commentator or announcer. He is wearing a white shirt and shorts, which is typical attire for a tennis player or official. The man on the right is seated on the edge of the court, holding a tennis racket and smiling, possibly a player or a coach. He is wearing a white shirt and black shorts. In the background, there is a fence separating the court from the spectator area, and beyond the fence, there are trees and buildings, indicating that the court is part of a larger sports complex or club. The sky is clear, suggesting it might be a sunny day. The image has a vintage or retro feel due to the black and white filter and the style of the clothing and the court's design. The text "THE FIRST ANNUAL WEST SIDE TENNIS CLUB" and "EVIAN RACQUET CUP 2012" are visible, indicating that this is an event sponsored by Evian, a brand known for its water products. The date "AUG 12" is also visible, which is likely the date of the event. The overall atmosphere of the image is casual and relaxed, with the focus on the tennis court and the people involved in the event.

**VLM response w/ svp:**

A man holding a tennis racket.

**Instruction:** Provide a short description for this region.



**VLM response w/o svp:**  
The pizza is in a box.

**VLM response w/ svp:**  
A slice of pizza.

**Instruction:** Provide a short description for this region.



**VLM response w/o svp:**  
This is a photo of a man riding a motorcycle with a dog sitting on the back. The man is wearing a black helmet and a black vest, and the dog appears to be a golden retriever. The man is also wearing a black tank top and blue jeans. The motorcycle is black and has a large engine. The setting appears to be an outdoor event or gathering, as there are other motorcycles parked in the background and a yellow police tape is visible in the foreground. The man is taking a photo of the scene with his cell phone.

**VLM response w/ svp:**  
A man taking a picture of a dog sitting on a motorcycle.

**Instruction:** What activity could potentially be enjoyed near the area shown in the image?



**VLM response:**

The image shows a wooden bench situated near a body of water, possibly a lake or a river. Given the serene and peaceful setting, one could potentially enjoy various activities such as: Sitting on the bench to relax, read a book, or simply enjoy the view of the water and the surrounding landscape. Taking a leisurely walk or jog along the water's edge, enjoying the tranquility and the natural beauty of the area. Engaging in photography, capturing the picturesque scenery and the reflections on the water's surface. Bird watching, as the area might be home to various bird species. Fishing, if the water body is a lake or a river with fish populations. Picnicking with friends or family, enjoying a meal outdoors in the fresh air and the calming presence of the water. These activities are suitable for the setting depicted in the image, offering a chance to unwind and connect with nature.

**Instruction:** What are some factors contributing to the difficulty of this activity?



**VLM response:**

The image shows a person skiing on a steep, snow-covered slope. The difficulty of this activity can be attributed to several factors: **Terrain:** The steepness of the slope increases the challenge of maintaining balance and control while skiing. Steeper slopes require more advanced skiing techniques and greater physical strength. **Snow Conditions:** The type of snow can greatly affect the difficulty of skiing. In the image, the snow appears to be well-packed, which can make it harder to carve turns and maintain speed. **Visibility:** The image shows a cloudy day, which can reduce visibility and make it more difficult to navigate the slope. **Equipment:** The skier is wearing a backpack, which can add extra weight and affect balance and maneuverability. **Weather:** The cloudy day suggests that the weather conditions might be challenging, with the possibility of poor visibility, cold temperatures, or even snowfall. **Skill Level:** The skier's skill level plays a significant role in the difficulty of the activity. More advanced skiers are better equipped to handle steep slopes and challenging

### I.3. Visual Queries



## J. Details

### J.1. Datasets

Dataset	Task	Split	$N$
<i>Sampling</i> COCO2014 [59]	VP	train	100:10000
<i>Evaluation</i> ScienceQA [81]	VQA	test	4241
VQAv2 [30]	VQA	val_lite	500
GQA [40]	VQA	lite	500
COCO2017 [59]	Captioning	val_lite	500
Flickr30k [75]	Captioning	test_lite	500
NoCaps [2]	Captioning	val_lite	500
COCO2014 [59]	Captioning	val	40504
COCO2017 [59]	Captioning	val	5000
Flickr30k [75]	Captioning	test	31783
NoCaps [2]	Captioning	val	4500
RefCOCO [46]	REG	val_lite	500
RefCOCO [46]	REG	val	8811
RefCOCO [46]	REG	test	5000
RefCOCO [46]	REG	testA	1975
RefCOCO [46]	REG	testB	1810
RefCOCO+ [46]	REG	val	3805
RefCOCO+ [46]	REG	testA	1975
RefCOCO+ [46]	REG	testB	1798
RefCOCOg [46]	REG	val	7573
RefCOCOg [46]	REG	test	5023
MMBench [64]	Multitasking	en_dev_lite	500
MMMU [116]	Multitasking	val	900
POPE [56]	Hallucinations	adv	3000
POPE [56]	Hallucinations	pop	3000
POPE [56]	Hallucinations	random	3000

Table 15. Datasets utilized in *SVP*. We use COCO2014 images as conditioning for building visual projections, using self-captioning and grounding feedback. VP: visual projection. VQA: visual question answering. REG: referring expression generation. We use `lmms-eval` [123] for all the evaluations. The `lite` splits as proposed in [123].

## J.2. Experiments

	LLaVA-1.5-13b	LLaVA-1.6-7b	LLaVA-1.6-13b	LLaVA-OV-0.5b	LLaVA-OV-7b
<i>Sampling</i>					
images	1000	1000	1000	2000	2000
iterations	1	1	1	1	1
prompt-version	llava_v1	mistral_instruct	llava_v1	qwen_1_5	qwen_1_5
sample-batch	20	20	20	10	10
samples/image	20	20	20	10	10
top $k$	0.2	0.2	0.2	0.1	0.1
<i>Training</i>					
accelerators	A100	A100	A100	A100	A100
deepspeed	w/ ZeRO-2	w/ ZeRO-3	w/ ZeRO-3	w/ ZeRO-3	w/ ZeRO-3
epochs	1	1	1	3	3
grad-acc	1	1	1	2	2
learning-rate	$2e^{-4}$	$2e^{-4}$	$2e^{-4}$	$1e^{-5}$	$1e^{-5}$
lora	w/	w/	w/	w/ and w/o	w/ and w/o
lora- $\alpha$	256	16	256	16	16
lora-r	128	64	128	64	64
lr-schedule	cos	cos	cos	cos	cos
max-tokens	2048	2048	2048	1024	1024
mix-precision	w/	w/	w/	w/	w/
optimizer	AdamW	AdamW	AdamW	AdamW	AdamW
samples	4000:8000	4000:8000	4000:8000	2000	2000
text-encoder	Vicuna-13b-v1.5	Mistral-7b-Instruct-v0.2	Vicuna-13b-v1.5	Qwen2-0.5b	Qwen2-7b
train-batch	16	16	16	4	4
vision-encoder	CLIP-L/14	CLIP-L/14	CLIP-L/14	SigLIP-SO/14	SigLIP-SO/14
warm-up-rate	0.03	0.03	0.03	0.03	0.03

Table 16. Hyper-parameters for the main experiments.

## References

- [1] Josh Achiam, Steven Adler, Sandhini Agarwal, Lama Ahmad, Ilge Akkaya, Florencia Leoni Aleman, Diogo Almeida, Janko Altenschmidt, Sam Altman, Shyamal Anadkat, et al. Gpt-4 technical report. *arXiv preprint arXiv:2303.08774*, 2023. 16
- [2] Harsh Agrawal, Karan Desai, Yufei Wang, Xinlei Chen, Rishabh Jain, Mark Johnson, Dhruv Batra, Devi Parikh, Stefan Lee, and Peter Anderson. Nocaps: Novel object captioning at scale. In *Proceedings of the IEEE/CVF international conference on computer vision*, pages 8948–8957, 2019. 6, 41
- [3] Ekin Akyürek, Dale Schuurmans, Jacob Andreas, Tengyu Ma, and Denny Zhou. What learning algorithm is in-context learning? investigations with linear models. *arXiv preprint arXiv:2211.15661*, 2022. 16
- [4] Michael L Anderson. Neural reuse: A fundamental organizational principle of the brain. *Behavioral and brain sciences*, 33(4): 245–266, 2010. 3, 16
- [5] Thomas Anthony, Zheng Tian, and David Barber. Thinking fast and slow with deep learning and tree search. *Advances in neural information processing systems*, 30, 2017. 2, 16
- [6] Yuntao Bai, Saurav Kadavath, Sandipan Kundu, Amanda Askell, Jackson Kernion, Andy Jones, Anna Chen, Anna Goldie, Azalia Mirhoseini, Cameron McKinnon, et al. Constitutional ai: Harmlessness from ai feedback. *arXiv preprint arXiv:2212.08073*, 2022. 16
- [7] Zechen Bai, Pichao Wang, Tianjun Xiao, Tong He, Zongbo Han, Zheng Zhang, and Mike Zheng Shou. Hallucination of multimodal large language models: A survey. *arXiv preprint arXiv:2404.18930*, 2024. 2
- [8] Satyanjeev Banerjee and Alon Lavie. Meteor: An automatic metric for mt evaluation with improved correlation with human judgments. In *Proceedings of the acl workshop on intrinsic and extrinsic evaluation measures for machine translation and/or summarization*, pages 65–72, 2005. 6
- [9] Lawrence W Barsalou. Grounded cognition. *Annu. Rev. Psychol.*, 59(1):617–645, 2008. 3, 16
- [10] Robert Bassett and Julio Deride. Maximum a posteriori estimators as a limit of bayes estimators. *Mathematical Programming*, 174: 129–144, 2019. 27
- [11] Lucas Beyer, Andreas Steiner, André Susano Pinto, Alexander Kolesnikov, Xiao Wang, Daniel Salz, Maxim Neumann, Ibrahim Alabdulmohsin, Michael Tschannen, Emanuele Bugliarello, et al. Paligemma: A versatile 3b vlm for transfer. *arXiv preprint arXiv:2407.07726*, 2024. 2, 3, 16
- [12] Florian Bordes, Richard Yuanzhe Pang, Anurag Ajay, Alexander C Li, Adrien Bardes, Suzanne Petryk, Oscar Mañas, Zhiqiu Lin, Anas Mahmoud, Bargav Jayaraman, et al. An introduction to vision-language modeling. *arXiv preprint arXiv:2405.17247*, 2024. 1
- [13] Ralph Allan Bradley and Milton E Terry. Rank analysis of incomplete block designs: I. the method of paired comparisons. *Biometrika*, 39(3/4):324–345, 1952. 30
- [14] Tom B. Brown, Benjamin Mann, Nick Ryder, Melanie Subbiah, Jared Kaplan, Prafulla Dhariwal, Arvind Neelakantan, Pranav Shyam, Girish Sastry, Amanda Askell, Sandhini Agarwal, Ariel Herbert-Voss, Gretchen Krueger, Tom Henighan, Rewon Child, Aditya Ramesh, Daniel M. Ziegler, Jeffrey Wu, Clemens Winter, Christopher Hesse, Mark Chen, Eric Sigler, Mateusz Litwin, Scott Gray, Benjamin Chess, Jack Clark, Christopher Berner, Sam McCandlish, Alec Radford, Ilya Sutskever, and Dario Amodei. Language models are few-shot learners. 2020. 1, 16
- [15] Yuri Burda, Harri Edwards, Deepak Pathak, Amos Storkey, Trevor Darrell, and Alexei A Efros. Large-scale study of curiosity-driven learning. *arXiv preprint arXiv:1808.04355*, 2018. 4
- [16] Nicolas Carion, Francisco Massa, Gabriel Synnaeve, Nicolas Usunier, Alexander Kirillov, and Sergey Zagoruyko. End-to-end object detection with transformers. In *European conference on computer vision*, pages 213–229. Springer, 2020. 3, 16
- [17] Zhe Chen, Weiyun Wang, Hao Tian, Shenglong Ye, Zhangwei Gao, Erfei Cui, Wenwen Tong, Kongzhi Hu, Jiapeng Luo, Zheng Ma, et al. How far are we to gpt-4v? closing the gap to commercial multimodal models with open-source suites. *arXiv preprint arXiv:2404.16821*, 2024. 1, 3
- [18] Zhe Chen, Jiannan Wu, Wenhai Wang, Weijie Su, Guo Chen, Sen Xing, Muyan Zhong, Qinglong Zhang, Xizhou Zhu, Lewei Lu, et al. Internvl: Scaling up vision foundation models and aligning for generic visual-linguistic tasks. In *Proceedings of the IEEE/CVF Conference on Computer Vision and Pattern Recognition*, pages 24185–24198, 2024. 5, 8, 19
- [19] Wei-Lin Chiang, Zhuohan Li, Zi Lin, Ying Sheng, Zhanghao Wu, Hao Zhang, Lianmin Zheng, Siyuan Zhuang, Yonghao Zhuang, Joseph E Gonzalez, et al. Vicuna: An open-source chatbot impressing gpt-4 with 90%\* chatgpt quality. See <https://vicuna.lmsys.org> (accessed 14 April 2023), 2(3):6, 2023. 5, 16
- [20] Paul F Christiano, Jan Leike, Tom Brown, Miljan Martic, Shane Legg, and Dario Amodei. Deep reinforcement learning from human preferences. *Advances in neural information processing systems*, 30, 2017. 2, 16, 30
- [21] Daniel Collerton, James Barnes, Nico J Diederich, Rob Dudley, Karl Friston, Christopher G Goetz, Jennifer G Goldman, Renaud Jardri, Jaime Kulisevsky, Simon JG Lewis, et al. Understanding visual hallucinations: A new synthesis. *Neuroscience & Biobehavioral Reviews*, 150:105208, 2023. 2
- [22] Wenliang Dai, Junnan Li, Dongxu Li, Anthony Meng Huat Tiong, Junqi Zhao, Weisheng Wang, Boyang Li, Pascale Fung, and Steven Hoi. Instructblip: Towards general-purpose vision-language models with instruction tuning, 2023. 20
- [23] Achal Dave, Piotr Dollár, Deva Ramanan, Alexander Kirillov, and Ross Girshick. Evaluating large-vocabulary object detectors: The devil is in the details. *arXiv preprint arXiv:2102.01066*, 2021. 3, 16

- [24] Hanze Dong, Wei Xiong, Deepanshu Goyal, Yihan Zhang, Winnie Chow, Rui Pan, Shizhe Diao, Jipeng Zhang, Kashun Shum, and Tong Zhang. Raft: Reward ranked finetuning for generative foundation model alignment. *arXiv preprint arXiv:2304.06767*, 2023. [16](#), [30](#)
- [25] Alexey Dosovitskiy, Lucas Beyer, Alexander Kolesnikov, Dirk Weissenborn, Xiaohua Zhai, Thomas Unterthiner, Mostafa Dehghani, Matthias Minderer, Georg Heigold, Sylvain Gelly, et al. An image is worth 16x16 words: Transformers for image recognition at scale. *arXiv preprint arXiv:2010.11929*, 2020. [1](#), [5](#)
- [26] Alessandro Favero, Luca Zancato, Matthew Trager, Siddharth Choudhary, Pramuditha Perera, Alessandro Achille, Ashwin Swaminathan, and Stefano Soatto. Multi-modal hallucination control by visual information grounding. In *Proceedings of the IEEE/CVF Conference on Computer Vision and Pattern Recognition*, pages 14303–14312, 2024. [2](#), [3](#), [16](#), [20](#)
- [27] Chelsea Finn, Pieter Abbeel, and Sergey Levine. Model-agnostic meta-learning for fast adaptation of deep networks. *70:1126–1135*, 2017. [16](#)
- [28] Ross Girshick, Jeff Donahue, Trevor Darrell, and Jitendra Malik. Rich feature hierarchies for accurate object detection and semantic segmentation. In *Proceedings of the IEEE conference on computer vision and pattern recognition*, pages 580–587, 2014. [3](#), [16](#)
- [29] Arthur M Glenberg and Michael P Kaschak. Grounding language in action. *Psychonomic bulletin & review*, 9(3):558–565, 2002. [3](#), [16](#)
- [30] Yash Goyal, Tejas Khot, Douglas Summers-Stay, Dhruv Batra, and Devi Parikh. Making the v in vqa matter: Elevating the role of image understanding in visual question answering. In *Proceedings of the IEEE conference on computer vision and pattern recognition*, pages 6904–6913, 2017. [6](#), [41](#)
- [31] Erin Grant, Chelsea Finn, Sergey Levine, Trevor Darrell, and Thomas L. Griffiths. Recasting gradient-based meta-learning as hierarchical bayes. 2018. [27](#)
- [32] Caglar Gulcehre, Tom Le Paine, Srivatsan Srinivasan, Ksenia Konyushkova, Lotte Weerts, Abhishek Sharma, Aditya Siddhant, Alex Ahern, Miaosen Wang, Chenjie Gu, et al. Reinforced self-training (rest) for language modeling. *arXiv preprint arXiv:2308.08998*, 2023. [2](#), [16](#), [30](#)
- [33] Agrim Gupta, Piotr Dollar, and Ross Girshick. Lvis: A dataset for large vocabulary instance segmentation. In *Proceedings of the IEEE/CVF conference on computer vision and pattern recognition*, pages 5356–5364, 2019. [3](#), [16](#)
- [34] John Hattie and Helen Timperley. The power of feedback. *Review of educational research*, 77(1):81–112, 2007. [2](#)
- [35] Yuting He, Fuxiang Huang, Xinrui Jiang, Yuxiang Nie, Minghao Wang, Jiguang Wang, and Hao Chen. Foundation model for advancing healthcare: Challenges, opportunities, and future directions. *arXiv preprint arXiv:2404.03264*, 2024. [2](#)
- [36] Matthew Douglas Hoffman, Du Phan, David Dohan, Sholto Douglas, Tuan Anh Le, Aaron Parisi, Pavel Sountsov, Charles Sutton, Sharad Vikram, and Rif A Saurous. Training chain-of-thought via latent-variable inference. *Advances in Neural Information Processing Systems*, 36, 2024. [4](#), [30](#)
- [37] Alex Holub, Pietro Perona, and Michael C Burl. Entropy-based active learning for object recognition. In *2008 IEEE Computer Society Conference on Computer Vision and Pattern Recognition Workshops*, pages 1–8. IEEE, 2008. [4](#)
- [38] Timothy Hospedales, Antreas Antoniou, Paul Micaelli, and Amos Storkey. Meta-learning in neural networks: A survey. *ArXiv preprint*, abs/2004.05439, 2020. [5](#), [16](#)
- [39] Edward J Hu, Yelong Shen, Phillip Wallis, Zeyuan Allen-Zhu, Yuanzhi Li, Shean Wang, Lu Wang, and Weizhu Chen. Lora: Low-rank adaptation of large language models. *arXiv preprint arXiv:2106.09685*, 2021. [3](#), [5](#), [6](#)
- [40] Drew A Hudson and Christopher D Manning. Gqa: A new dataset for real-world visual reasoning and compositional question answering. In *Proceedings of the IEEE/CVF conference on computer vision and pattern recognition*, pages 6700–6709, 2019. [6](#), [41](#)
- [41] Hamish Ivison, Yizhong Wang, Jiacheng Liu, Zeqiu Wu, Valentina Pyatkin, Nathan Lambert, Noah A Smith, Yejin Choi, and Hannaneh Hajishirzi. Unpacking dpo and ppo: Disentangling best practices for learning from preference feedback. *arXiv preprint arXiv:2406.09279*, 2024. [31](#)
- [42] Albert Q Jiang, Alexandre Sablayrolles, Arthur Mensch, Chris Bamford, Devendra Singh Chaplot, Diego de las Casas, Florian Bressand, Gianna Lengyel, Guillaume Lample, Lucile Saulnier, et al. Mistral 7b. *arXiv preprint arXiv:2310.06825*, 2023. [5](#)
- [43] Michael I Jordan, Zoubin Ghahramani, Tommi S Jaakkola, and Lawrence K Saul. An introduction to variational methods for graphical models. *Machine learning*, 37(2):183–233, 1999. [4](#), [27](#)
- [44] Junmo Kang, Leonid Karlinsky, Hongyin Luo, Zhen Wang, Jacob Hansen, James Glass, David Cox, Rameswar Panda, Rogerio Feris, and Alan Ritter. Self-moe: Towards compositional large language models with self-specialized experts. *arXiv preprint arXiv:2406.12034*, 2024. [16](#)
- [45] Junmo Kang, Hongyin Luo, Yada Zhu, Jacob Hansen, James Glass, David Cox, Alan Ritter, Rogerio Feris, and Leonid Karlinsky. Self-specialization: Uncovering latent expertise within large language models. In *Findings of the Association for Computational Linguistics ACL 2024*, pages 2681–2706, 2024. [16](#)
- [46] Sahar Kazemzadeh, Vicente Ordonez, Mark Matten, and Tamara Berg. Referitgame: Referring to objects in photographs of natural scenes. In *Proceedings of the 2014 conference on empirical methods in natural language processing (EMNLP)*, pages 787–798, 2014. [6](#), [33](#), [41](#)
- [47] Markus Kiefer and Lawrence W Barsalou. Grounding the human conceptual system in perception, action, and internal states. 2013. [3](#), [16](#)

- [48] Diederik P. Kingma and Max Welling. Auto-encoding variational bayes. 2014. 4
- [49] Diederik P Kingma and Max Welling. An introduction to variational autoencoders. *arXiv preprint arXiv:1906.02691*, 2019. 4, 27
- [50] Black Forest Labs. Flux. <https://github.com/black-forest-labs/flux>, 2024. 12, 13, 14
- [51] Sicong Leng, Hang Zhang, Guanzheng Chen, Xin Li, Shijian Lu, Chunyan Miao, and Lidong Bing. Mitigating object hallucinations in large vision-language models through visual contrastive decoding. In *Proceedings of the IEEE/CVF Conference on Computer Vision and Pattern Recognition*, pages 13872–13882, 2024. 2, 3, 16, 20
- [52] Bo Li, Yuanhan Zhang, Dong Guo, Renrui Zhang, Feng Li, Hao Zhang, Kaichen Zhang, Yanwei Li, Ziwei Liu, and Chunyuan Li. Llava-onevision: Easy visual task transfer. *arXiv preprint arXiv:2408.03326*, 2024. 1, 3, 5, 6, 8, 19
- [53] Junnan Li, Dongxu Li, Caiming Xiong, and Steven Hoi. Blip: Bootstrapping language-image pre-training for unified vision-language understanding and generation. In *ICML*, 2022. 1, 3, 4
- [54] Junnan Li, Dongxu Li, Silvio Savarese, and Steven Hoi. Blip-2: Bootstrapping language-image pre-training with frozen image encoders and large language models. In *International conference on machine learning*, pages 19730–19742. PMLR, 2023. 11
- [55] Liunian Harold Li, Pengchuan Zhang, Haotian Zhang, Jianwei Yang, Chunyuan Li, Yiwu Zhong, Lijuan Wang, Lu Yuan, Lei Zhang, Jenq-Neng Hwang, et al. Grounded language-image pre-training. In *Proceedings of the IEEE/CVF Conference on Computer Vision and Pattern Recognition*, pages 10965–10975, 2022. 3, 16
- [56] Yifan Li, Yifan Du, Kun Zhou, Jinpeng Wang, Wayne Xin Zhao, and Ji-Rong Wen. Evaluating object hallucination in large vision-language models. *arXiv preprint arXiv:2305.10355*, 2023. 6, 41
- [57] Chin-Yew Lin. Rouge: A package for automatic evaluation of summaries. In *Text summarization branches out*, pages 74–81, 2004. 6
- [58] Ji Lin, Hongxu Yin, Wei Ping, Pavlo Molchanov, Mohammad Shoeybi, and Song Han. Vila: On pre-training for visual language models. In *Proceedings of the IEEE/CVF Conference on Computer Vision and Pattern Recognition*, pages 26689–26699, 2024. 5, 8, 19
- [59] Tsung-Yi Lin, Michael Maire, Serge Belongie, James Hays, Pietro Perona, Deva Ramanan, Piotr Dollár, and C Lawrence Zitnick. Microsoft coco: Common objects in context. In *Computer Vision—ECCV 2014: 13th European Conference, Zurich, Switzerland, September 6-12, 2014, Proceedings, Part V 13*, pages 740–755. Springer, 2014. 3, 5, 6, 16, 25, 33, 41
- [60] Haotian Liu, Chunyuan Li, Yuheng Li, and Yong Jae Lee. Improved baselines with visual instruction tuning. In *Proceedings of the IEEE/CVF Conference on Computer Vision and Pattern Recognition*, pages 26296–26306, 2024. 2, 3, 5, 8, 16, 19
- [61] Haotian Liu, Chunyuan Li, Yuheng Li, Bo Li, Yuanhan Zhang, Sheng Shen, and Yong Jae Lee. Llava-next: Improved reasoning, ocr, and world knowledge, 2024. 4, 5, 6, 8, 19, 20
- [62] Haotian Liu, Chunyuan Li, Qingyang Wu, and Yong Jae Lee. Visual instruction tuning. *Advances in neural information processing systems*, 36, 2024. 8, 19
- [63] Shilong Liu, Zhaoyang Zeng, Tianhe Ren, Feng Li, Hao Zhang, Jie Yang, Chunyuan Li, Jianwei Yang, Hang Su, Jun Zhu, et al. Grounding dino: Marrying dino with grounded pre-training for open-set object detection. *arXiv preprint arXiv:2303.05499*, 2023. 2, 3, 5, 6, 11, 16
- [64] Yuan Liu, Haodong Duan, Yuanhan Zhang, Bo Li, Songyang Zhang, Wangbo Zhao, Yike Yuan, Jiaqi Wang, Conghui He, Ziwei Liu, et al. Mmbench: Is your multi-modal model an all-around player? In *European Conference on Computer Vision*, pages 216–233. Springer, 2025. 6, 41
- [65] Aman Madaan, Niket Tandon, Prakhar Gupta, Skyler Hallinan, Luyu Gao, Sarah Wiegrefe, Uri Alon, Nouha Dziri, Shrimai Prabhumoye, Yiming Yang, et al. Self-refine: Iterative refinement with self-feedback. *Advances in Neural Information Processing Systems*, 36, 2024. 16
- [66] Chris J Maddison, Andriy Mnih, and Yee Whye Teh. The concrete distribution: A continuous relaxation of discrete random variables. *arXiv preprint arXiv:1611.00712*, 2016. 4
- [67] Ilya Nemenman, Fariel Shafee, and William Bialek. Entropy and inference, revisited. *Advances in neural information processing systems*, 14, 2001. 5
- [68] Maxime Oquab, Leon Bottou, Ivan Laptev, and Josef Sivic. Learning and transferring mid-level image representations using convolutional neural networks. In *Proceedings of the IEEE conference on computer vision and pattern recognition*, pages 1717–1724, 2014. 2
- [69] Long Ouyang, Jeff Wu, Xu Jiang, Diogo Almeida, Carroll L Wainwright, Pamela Mishkin, Chong Zhang, Sandhini Agarwal, Katarina Slama, Alex Ray, et al. Training language models to follow instructions with human feedback. *arXiv preprint arXiv:2203.02155*, 2022. 2, 3, 16
- [70] Kishore Papineni, Salim Roukos, Todd Ward, and Wei-Jing Zhu. Bleu: a method for automatic evaluation of machine translation. In *Proceedings of the 40th annual meeting of the Association for Computational Linguistics*, pages 311–318, 2002. 6
- [71] Deepak Pathak, Pulkit Agrawal, Alexei A Efros, and Trevor Darrell. Curiosity-driven exploration by self-supervised prediction. In *International conference on machine learning*, pages 2778–2787. PMLR, 2017. 4
- [72] Jonathan W Peirce. Understanding mid-level representations in visual processing. *Journal of Vision*, 15(7):5–5, 2015. 2
- [73] Zhiliang Peng, Wenhui Wang, Li Dong, Yaru Hao, Shaohan Huang, Shuming Ma, Qixiang Ye, and Furu Wei. Grounding multimodal large language models to the world. In *The Twelfth International Conference on Learning Representations*, 2024. 2, 3, 16

- [74] Cyril Picard, Kristen M Edwards, Anna C Doris, Brandon Man, Giorgio Giannone, Md Ferdous Alam, and Faez Ahmed. From concept to manufacturing: Evaluating vision-language models for engineering design. *arXiv preprint arXiv:2311.12668*, 2023. [2](#)
- [75] Bryan A Plummer, Liwei Wang, Chris M Cervantes, Juan C Caicedo, Julia Hockenmaier, and Svetlana Lazebnik. Flickr30k entities: Collecting region-to-phrase correspondences for richer image-to-sentence models. In *Proceedings of the IEEE international conference on computer vision*, pages 2641–2649, 2015. [6](#), [41](#)
- [76] Alec Radford, Jeffrey Wu, Rewon Child, David Luan, Dario Amodei, Ilya Sutskever, et al. Language models are unsupervised multitask learners. *OpenAI blog*, 1(8):9, 2019. [5](#)
- [77] Alec Radford, Jong Wook Kim, Chris Hallacy, Aditya Ramesh, Gabriel Goh, Sandhini Agarwal, Girish Sastry, Amanda Askell, Pamela Mishkin, Jack Clark, et al. Learning transferable visual models from natural language supervision. In *International Conference on Machine Learning*, pages 8748–8763. PMLR, 2021. [1](#), [5](#)
- [78] Rafael Rafailov, Archit Sharma, Eric Mitchell, Christopher D Manning, Stefano Ermon, and Chelsea Finn. Direct preference optimization: Your language model is secretly a reward model. *Advances in Neural Information Processing Systems*, 36, 2024. [2](#), [3](#), [9](#), [16](#), [20](#), [25](#), [30](#), [31](#)
- [79] Pooyan Rahmanzadehgervi, Logan Bolton, Mohammad Reza Taesiri, and Anh Totti Nguyen. Vision language models are blind. *arXiv preprint arXiv:2407.06581*, 2024. [1](#)
- [80] J Redmon. You only look once: Unified, real-time object detection. In *Proceedings of the IEEE conference on computer vision and pattern recognition*, 2016. [3](#), [16](#)
- [81] Tanik Saikh, Tirthankar Ghosal, Amish Mittal, Asif Ekbal, and Pushpak Bhattacharyya. Scienceqa: A novel resource for question answering on scholarly articles. *International Journal on Digital Libraries*, 23(3):289–301, 2022. [6](#), [41](#)
- [82] Kuleen Sasse, Shan Chen, Jackson Pond, Danielle Bitterman, and John Osborne. Mapping bias in vision language models: Signposts, pitfalls, and the road ahead. *arXiv preprint arXiv:2410.13146*, 2024. [1](#)
- [83] Tom Schaul and Jürgen Schmidhuber. Metalearning. *Scholarpedia*, 5(6):4650, 2010. [16](#)
- [84] Jürgen Schmidhuber. *Evolutionary principles in self-referential learning, or on learning how to learn: the meta-meta-... hook*. PhD thesis, Technische Universität München, 1987. [16](#)
- [85] Juergen Schmidhuber. A general method for incremental self-improvement and multi-agent learning. In *Evolutionary Computation: Theory and Applications*, pages 81–123. World Scientific, 1999. [16](#)
- [86] John Schulman, Filip Wolski, Prafulla Dhariwal, Alec Radford, and Oleg Klimov. Proximal policy optimization algorithms. *arXiv preprint arXiv:1707.06347*, 2017. [30](#)
- [87] Burr Settles. Active learning literature survey. 2009. [4](#)
- [88] Noah Shinn, Federico Cassano, Ashwin Gopinath, Karthik Narasimhan, and Shunyu Yao. Reflexion: Language agents with verbal reinforcement learning. *Advances in Neural Information Processing Systems*, 36, 2024. [16](#)
- [89] David Silver, Aja Huang, Chris J Maddison, Arthur Guez, Laurent Sifre, George Van Den Driessche, Julian Schrittwieser, Ioannis Antonoglou, Veda Panneershelvam, Marc Lanctot, et al. Mastering the game of go with deep neural networks and tree search. *nature*, 529(7587):484–489, 2016. [16](#)
- [90] David Silver, Julian Schrittwieser, Karen Simonyan, Ioannis Antonoglou, Aja Huang, Arthur Guez, Thomas Hubert, Lucas Baker, Matthew Lai, Adrian Bolton, et al. Mastering the game of go without human knowledge. *nature*, 550(7676):354–359, 2017. [16](#)
- [91] Binyang Song, Rui Zhou, and Faez Ahmed. Multi-modal machine learning in engineering design: A review and future directions. *Journal of Computing and Information Science in Engineering*, 24(1):010801, 2024. [2](#)
- [92] Shivchander Sudalairaj, Abhishek Bhandwalidar, Aldo Pareja, Kai Xu, David D Cox, and Akash Srivastava. Lab: Large-scale alignment for chatbots. *arXiv preprint arXiv:2403.01081*, 2024. [16](#)
- [93] Zhiqing Sun, Sheng Shen, Shengcao Cao, Haotian Liu, Chunyuan Li, Yikang Shen, Chuang Gan, Liang-Yan Gui, Yu-Xiong Wang, Yiming Yang, et al. Aligning large multimodal models with factually augmented rlhf. *arXiv preprint arXiv:2309.14525*, 2023. [2](#), [3](#), [6](#), [8](#), [16](#), [19](#), [20](#)
- [94] Zhiqing Sun, Yikang Shen, Qinhong Zhou, Hongxin Zhang, Zhenfang Chen, David Cox, Yiming Yang, and Chuang Gan. Principle-driven self-alignment of language models from scratch with minimal human supervision. *Advances in Neural Information Processing Systems*, 36, 2024. [16](#)
- [95] Gershon Tenenbaum and Ellen Goldring. A meta-analysis of the effect of enhanced instruction: cues, participation, reinforcement and feedback and correctives on motor skill learning. *Journal of Research & Development in Education*, 1989. [2](#)
- [96] Joshua B Tenenbaum, Charles Kemp, Thomas L Griffiths, and Noah D Goodman. How to grow a mind: Statistics, structure, and abstraction. *science*, 331(6022):1279–1285, 2011. [2](#)
- [97] Shengbang Tong, Ellis Brown, Penghao Wu, Sanghyun Woo, Manoj Middepogu, Sai Charitha Akula, Jihan Yang, Shusheng Yang, Adithya Iyer, Xichen Pan, et al. Cambrian-1: A fully open, vision-centric exploration of multimodal llms. *arXiv preprint arXiv:2406.16860*, 2024. [3](#), [16](#)
- [98] Hugo Touvron, Thibaut Lavril, Gautier Izacard, Xavier Martinet, Marie-Anne Lachaux, Timothée Lacroix, Baptiste Rozière, Naman Goyal, Eric Hambro, Faisal Azhar, et al. Llama: Open and efficient foundation language models. *arXiv preprint arXiv:2302.13971*, 2023. [1](#)

- [99] Giuseppe Vallar. Spatial neglect, balint-homes' and gerstmann's syndrome, and other spatial disorders. *Cns Spectrums*, 12(7): 527–536, 2007. [2](#)
- [100] Ashish Vaswani, Noam Shazeer, Niki Parmar, Jakob Uszkoreit, Llion Jones, Aidan N. Gomez, Lukasz Kaiser, and Illia Polosukhin. Attention is all you need. In *Advances in Neural Information Processing Systems 30: Annual Conference on Neural Information Processing Systems 2017, December 4-9, 2017, Long Beach, CA, USA*, pages 5998–6008, 2017. [4](#)
- [101] Ramakrishna Vedantam, C Lawrence Zitnick, and Devi Parikh. Cider: Consensus-based image description evaluation. In *Proceedings of the IEEE conference on computer vision and pattern recognition*, pages 4566–4575, 2015. [6](#)
- [102] David Wan, Jaemin Cho, Elias Stengel-Eskin, and Mohit Bansal. Contrastive region guidance: Improving grounding in vision-language models without training. *arXiv preprint arXiv:2403.02325*, 2024. [2](#), [3](#), [16](#)
- [103] Xuezhi Wang, Jason Wei, Dale Schuurmans, Quoc Le, Ed Chi, and Denny Zhou. Self-consistency improves chain of thought reasoning in language models. *arXiv preprint arXiv:2203.11171*, 2022. [16](#)
- [104] Xiyao Wang, Jiuhai Chen, Zhaoyang Wang, Yuhang Zhou, Yiyang Zhou, Huaxiu Yao, Tianyi Zhou, Tom Goldstein, Parminder Bhatia, Furong Huang, et al. Enhancing visual-language modality alignment in large vision language models via self-improvement. *arXiv preprint arXiv:2405.15973*, 2024. [16](#)
- [105] Jason Wei, Xuezhi Wang, Dale Schuurmans, Maarten Bosma, Ed Chi, Quoc Le, and Denny Zhou. Chain of thought prompting elicits reasoning in large language models. *arXiv preprint arXiv:2201.11903*, 2022. [4](#), [16](#)
- [106] Ronald J Williams. Simple statistical gradient-following algorithms for connectionist reinforcement learning. *Machine learning*, 8: 229–256, 1992. [31](#)
- [107] Sang Michael Xie, Aditi Raghunathan, Percy Liang, and Tengyu Ma. An explanation of in-context learning as implicit bayesian inference. *arXiv preprint arXiv:2111.02080*, 2021. [16](#)
- [108] Jiazheng Xu, Xiao Liu, Yuchen Wu, Yuxuan Tong, Qinkai Li, Ming Ding, Jie Tang, and Yuxiao Dong. Imagereward: Learning and evaluating human preferences for text-to-image generation. *Advances in Neural Information Processing Systems*, 36, 2024. [11](#)
- [109] An Yang, Baosong Yang, Binyuan Hui, Bo Zheng, Bowen Yu, Chang Zhou, Chengpeng Li, Chengyuan Li, Dayiheng Liu, Fei Huang, et al. Qwen2 technical report. *arXiv preprint arXiv:2407.10671*, 2024. [5](#)
- [110] Shunyu Yao, Jeffrey Zhao, Dian Yu, Nan Du, Izhak Shafran, Karthik Narasimhan, and Yuan Cao. React: Synergizing reasoning and acting in language models. *arXiv preprint arXiv:2210.03629*, 2022. [16](#)
- [111] Qinghao Ye, Haiyang Xu, Jiabo Ye, Ming Yan, Anwen Hu, Haowei Liu, Qi Qian, Ji Zhang, and Fei Huang. mplug-owl2: Revolutionizing multi-modal large language model with modality collaboration. In *Proceedings of the IEEE/CVF Conference on Computer Vision and Pattern Recognition*, pages 13040–13051, 2024. [1](#), [20](#)
- [112] Shukang Yin, Chaoyou Fu, Sirui Zhao, Tong Xu, Hao Wang, Dianbo Sui, Yunhang Shen, Ke Li, Xing Sun, and Enhong Chen. Woodpecker: Hallucination correction for multimodal large language models. *arXiv preprint arXiv:2310.16045*, 2023. [2](#), [3](#), [16](#), [20](#)
- [113] Haoxuan You, Haotian Zhang, Zhe Gan, Xianzhi Du, Bowen Zhang, Zirui Wang, Liangliang Cao, Shih-Fu Chang, and Yinfei Yang. Ferret: Refer and ground anything anywhere at any granularity. *arXiv preprint arXiv:2310.07704*, 2023. [2](#), [3](#), [16](#)
- [114] Alex Young, Bei Chen, Chao Li, Chengen Huang, Ge Zhang, Guanwei Zhang, Heng Li, Jiangcheng Zhu, Jianqun Chen, Jing Chang, et al. Yi: Open foundation models by 01. ai. *arXiv preprint arXiv:2403.04652*, 2024. [5](#)
- [115] Lu Yuan, Dongdong Chen, Yi-Ling Chen, Noel Codella, Xiyang Dai, Jianfeng Gao, Houdong Hu, Xuedong Huang, Boxin Li, Chunyuan Li, et al. Florence: A new foundation model for computer vision. *arXiv preprint arXiv:2111.11432*, 2021. [2](#), [3](#), [16](#)
- [116] Xiang Yue, Yuansheng Ni, Kai Zhang, Tianyu Zheng, Ruoqi Liu, Ge Zhang, Samuel Stevens, Dongfu Jiang, Weiming Ren, Yuxuan Sun, et al. Mmmu: A massive multi-discipline multimodal understanding and reasoning benchmark for expert agi. In *Proceedings of the IEEE/CVF Conference on Computer Vision and Pattern Recognition*, pages 9556–9567, 2024. [6](#), [41](#)
- [117] Eric Zelikman, Yuhuai Wu, Jesse Mu, and Noah Goodman. Star: Bootstrapping reasoning with reasoning. *Advances in Neural Information Processing Systems*, 35:15476–15488, 2022. [2](#), [4](#), [16](#), [30](#)
- [118] Eric Zelikman, Georges Harik, Yijia Shao, Varuna Jayasiri, Nick Haber, and Noah D Goodman. Quiet-star: Language models can teach themselves to think before speaking. *arXiv preprint arXiv:2403.09629*, 2024. [4](#), [16](#)
- [119] Xiaohua Zhai, Basil Mustafa, Alexander Kolesnikov, and Lucas Beyer. Sigmoid loss for language image pre-training. In *Proceedings of the IEEE/CVF International Conference on Computer Vision*, pages 11975–11986, 2023. [5](#)
- [120] Duzhen Zhang, Yahan Yu, Jiahua Dong, Chenxing Li, Dan Su, Chenhui Chu, and Dong Yu. Mm-llms: Recent advances in multimodal large language models. *arXiv preprint arXiv:2401.13601*, 2024. [1](#)
- [121] Hao Zhang, Feng Li, Shilong Liu, Lei Zhang, Hang Su, Jun Zhu, Lionel M Ni, and Heung-Yeung Shum. Dino: Detr with improved denoising anchor boxes for end-to-end object detection. *arXiv preprint arXiv:2203.03605*, 2022. [3](#), [16](#)
- [122] Hao Zhang, Hongyang Li, Feng Li, Tianhe Ren, Xueyan Zou, Shilong Liu, Shijia Huang, Jianfeng Gao, Chunyuan Li, Jainwei Yang, et al. Llava-grounding: Grounded visual chat with large multimodal models. In *European Conference on Computer Vision*, pages 19–35. Springer, 2025. [2](#), [3](#), [16](#)
- [123] Kaichen Zhang, Bo Li, Peiyuan Zhang, Fanyi Pu, Joshua Adrian Cahyono, Kairui Hu, Shuai Liu, Yuanhan Zhang, Jingkang Yang, Chunyuan Li, et al. Lmms-eval: Reality check on the evaluation of large multimodal models. *arXiv preprint arXiv:2407.12772*, 2024. [6](#), [8](#), [17](#), [18](#), [33](#), [41](#)

- [124] Zhiyuan Zhao, Bin Wang, Linke Ouyang, Xiaoyi Dong, Jiaqi Wang, and Conghui He. Beyond hallucinations: Enhancing lvlms through hallucination-aware direct preference optimization. *arXiv preprint arXiv:2311.16839*, 2023. [8](#), [19](#), [20](#)
- [125] Yiyang Zhou, Chenhang Cui, Rafael Rafailov, Chelsea Finn, and Huaxiu Yao. Aligning modalities in vision large language models via preference fine-tuning. *arXiv preprint arXiv:2402.11411*, 2024. [2](#), [3](#), [16](#)
- [126] Deyao Zhu, Jun Chen, Xiaoqian Shen, Xiang Li, and Mohamed Elhoseiny. Minigt-4: Enhancing vision-language understanding with advanced large language models. *arXiv preprint arXiv:2304.10592*, 2023. [4](#)
- [127] Ke Zhu, Liang Zhao, Zheng Ge, and Xiangyu Zhang. Self-supervised visual preference alignment. In *Proceedings of the 32nd ACM International Conference on Multimedia*, pages 291–300, 2024. [3](#), [6](#), [16](#), [20](#)
- [128] Daniel M Ziegler, Nisan Stiennon, Jeffrey Wu, Tom B Brown, Alec Radford, Dario Amodei, Paul Christiano, and Geoffrey Irving. Fine-tuning language models from human preferences. *arXiv preprint arXiv:1909.08593*, 2019. [30](#)